

T-4109

LIQUID PHASE SINTERING OF
 $\text{Al}_2\text{O}_3/\text{SiC}$ COMPOSITES

by
Wendy K. Hahn

ARTHUR LAKES LIBRARY
COLORADO SCHOOL OF MINES
GOLDEN, CO 80401

ProQuest Number: 10783759

All rights reserved

INFORMATION TO ALL USERS

The quality of this reproduction is dependent upon the quality of the copy submitted.

In the unlikely event that the author did not send a complete manuscript and there are missing pages, these will be noted. Also, if material had to be removed, a note will indicate the deletion.



ProQuest 10783759

Published by ProQuest LLC (2018). Copyright of the Dissertation is held by the Author.

All rights reserved.

This work is protected against unauthorized copying under Title 17, United States Code
Microform Edition © ProQuest LLC.

ProQuest LLC.
789 East Eisenhower Parkway
P.O. Box 1346
Ann Arbor, MI 48106 – 1346

T-4109

A thesis submitted to the Faculty and the Board of Trustees of the Colorado School of Mines in partial fulfillment of the requirements for the degree of Master of Science (Materials Science).

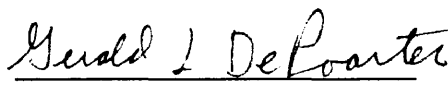
Golden, Colorado

Date 4/7/92

Signed:

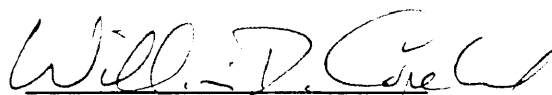

Wendy K. Hahn

Approved:


Dr. Gerald L. DePoorter
Thesis Advisor

Golden, Colorado

Date April 7, 1992


Dr. William D. Copeland
Professor and Coordinator,
Materials Science Program

ABSTRACT

Alumina/SiC composites are valuable materials for high temperature, high strength, high toughness and low density applications. However they are difficult to sinter unless a liquid phase is present during sintering. The liquid phase must not chemically react with the silicon carbide reinforcement, and for the best mechanical properties, the condensed liquid phase should devitrify.

The thermodynamics of reactions between various oxides and SiC were studied and two types of glass-ceramic frits were developed to act as a liquid phase sintering aid. These frits were incorporated into Al₂O₃/SiC platelet composites. The frits were composed of lithia-alumina-silicate and magnesia-alumina-silicate with titania as a nucleating agent.

Composites containing 85 wt% Al₂O₃, 10 wt% SiC, and 5 wt% glass were sintered at 1000°C in N₂, at 1400°C and 1500°C in Ar and at 1600°C under vacuum for 1 hr. Composites containing only the glass frits and 10 wt% SiC were also sintered at 1000°C in N₂ to test for reaction between the glass and platelets, and to determine whether additional heat treatment would be required to devitrify the glass-ceramic.

SEM examination of each of the composites found no evidence of platelet degradation due to chemical reaction between the glass and the SiC. X-ray diffraction analysis showed that most of the glass phase had devitrified.

Composites with each glass also were hot-pressed at 70 MPa (10,000 psi) and 1600°C under vacuum, to improve the densification rate. Each sintering aid improved the densities of the composites to 97% of theoretical density. X-ray diffraction analysis showed that all of the glass had devitrified in both composites. A composite with Al₂O₃ and SiC platelets without any sintering aids was hot-pressed at 1600°C and 70 MPa (10,000 psi) under vacuum for comparing the microstructure and density of the composites.

TABLE OF CONTENTS

| | <u>Page</u> |
|--|-------------|
| ABSTRACT | iii |
| LIST OF FIGURES | vii |
| LIST OF TABLES | ix |
| ACKNOWLEDGEMENTS | x |
| CHAPTER | |
| 1. INTRODUCTION | 1 |
| 2. SINTERING AID DEVELOPMENT | 9 |
| 2.1 Sintering Aid Selection Criteria | 9 |
| 2.2 Glass Formation | 13 |
| 2.3 Glass Devitrification and Glass Ceramics | 15 |
| 2.4 Thermodynamic Analysis | 17 |
| 2.5 Glass Ceramic Sintering Aid | 25 |
| 3. EXPERIMENTAL PROCEDURE | 29 |
| 3.1 Composite Preparation | 29 |
| 3.2 Composite Microstructural Evaluation | 34 |

4. RESULTS AND DISCUSSION 35

4.1 Glass-Ceramic Processing Evaluation 35

4.2 Alumina/SiC Composite Microstructural Evaluation 35

4.3 X-ray Diffraction of Alumina/SiC/Glass
Composites 47

4.4 Densification of Alumina/SiC/Glass Composites
by Sintering Aids 55

5. CONCLUSIONS 57

.....

REFERENCES 59

APPENDIX A 62

APPENDIX B 66

LIST OF FIGURES

| <u>Figure</u> | | <u>Page</u> |
|---------------|--|-------------|
| 1 | Crack deflection and retardation due to whiskers within the matrix | 6 |
| 2 | Surface of a SiC whisker in alumina with MnO ₂ -TiO ₂ flux | 8 |
| 3 | Ternary phase relationship of the LAS system | 11 |
| 4 | Ternary phase relationship of the MAS system | 12 |
| 5 | Volume-temperature relationships for glass and crystalline solids | 14 |
| 6 | Representation of the ordered crystalline and random network structure of glass | 15 |
| 7 | Temperature dependence of ΔG° for oxidation reactions of SiC | 18 |
| 8 | Temperature dependence of ΔG° for various metal carbides | 21 |
| 9 | Schematic and photograph of hot-press and furnace package | 33 |
| 10 | Differential Thermal Analysis of LAS | 36 |
| 11 | Differential Thermal Analysis of MAS | 37 |
| 12 | SiC platelets | 38 |
| 13 | LAS and MAS glass/SiC sintered at 1000°C | 39 |
| 14 | ASL and ASM sintered at 1000°C | 40 |
| 15 | ASL and ASM sintered at 1400°C | 41 |

| | | |
|----|---|----|
| 16 | ASL and ASM sintered at 1500°C | 42 |
| 17 | ASL and ASM sintered at 1600°C | 43 |
| 18 | ASL and ASM hot-pressed at 1600°C and 70 MPa | 45 |
| 19 | Alumina/SiC hot-pressed at 1600°C and 70 MPa | 46 |
| 20 | X-ray diffraction of LAS | 48 |
| 21 | X-ray diffraction of ASL | 49 |
| 22 | X-ray diffraction of ASL, hot-pressed | 50 |
| 23 | X-ray diffraction of MAS | 51 |
| 24 | X-ray diffraction of ASM | 52 |
| 25 | X-ray diffraction of ASM, hot-pressed | 53 |
| 26 | X-ray diffraction of alumina/SiC, hot-pressed | 54 |
| 27 | Density of alumina/SiC/glass composites | 56 |

LIST OF TABLES

| <u>Table</u> | | <u>Page</u> |
|--------------|---|-------------|
| 1 | COMPARISON OF THE STRENGTH AND TOUGHNESS OF MONOLITHIC ALUMINA AND ALUMINA MATRIX COMPOSITES . . | 3 |
| 2 | MECHANICAL PROPERTIES OF $\text{Al}_2\text{O}_3/10\text{wt}\%$ SiC WITH THE ADDITION OF $\text{TiO}_2/\text{MnO}_2$ SINTERING AID | 4 |
| 3 | SINTERING AID COMPOSITIONS | 10 |
| 4 | THERMODYNAMIC MODEL OF ALUMINA/SiC COMPOSITES AT 1800°K USING "SOLGASMIX" | 23 |
| 5 | COMPOSITE COMPOSITIONS | 25 |
| 6 | EXPERIMENTAL COMPOSITIONS AND PROCESS CONDITIONS . . . | 30 |

ACKNOWLEDGEMENTS

I would like to acknowledge the support of the Colorado Center for Advanced Ceramics and the Coors Ceramics Company for this project. I want to thank Dr. DePoorter for all of his help, advise, encouragement and support. I also appreciate the advice and assistance I have received from Dr. Brog, Dr. Wirth, Dr. Readey, Dr. Witters, Dr. Williamson and Dr. Haun. Thank you especially to my husband, Thad, for moving to Colorado so I could attend graduate school and for pushing me to keep going and finish.

LIQUID PHASE SINTERING OF $\text{Al}_2\text{O}_3/\text{SiC}$ COMPOSITES

CHAPTER 1

INTRODUCTION

Alumina-silicon carbide composites with high whisker/platelet loadings (≥ 10 wt%) generally must be hot-pressed at high temperatures and pressures to achieve near-theoretical density and therefore the highest strength and toughness. However, the hot pressing process limits the intricacy of the shape of the resulting parts and increases manufacturing costs. The goal for this research project was to find sintering aids which would allow the sintering of the composite to high density without reacting with the reinforcing phase of the composite and allow the pressure and temperature required for sintering to be reduced. Hot-pressing was used to prepare composites for evaluating the performance of the sintering aids. Eventually these sintering aids will be used to allow the composite to be prepared by sintering and hot isostatic pressing (HIPping). The applications for the composite would be greatly expanded through the production of more complex shapes and near-net-shape forming.

This project investigated the use of platelets in the composites in place of the more commonly used whiskers. The SiC whiskers are believed to have serious health effects^[1], similar to those of asbestos fibers. Platelets also have a lower defect density,

higher thermal stability and lower cost than whiskers^[2]. Tieg and Dillard found that whiskers with aspect ratios of 20:1 produced composites with higher green densities and sintered densities than composites prepared with whiskers having aspect ratios of 40:1^[3]. The aspect ratio (length/diameter or thickness, in the case of platelets) for platelets is approximately 10. Composites of Al₂O₃ and SiC platelets prepared by researchers at Alcan International and C-Axis Technology^[4] achieved nearly 100% theoretical density at 30 wt% platelet loading when hot pressed (1500°C at 124 MPa). They achieved strength and fracture toughness up to 360 MPa and 7.9 MPa·m^{1/2}, respectively.

A comparison of the reported strength and fracture toughness of high density alumina; alumina in which the glassy phase has been devitrified; alumina containing various particulate reinforcements; and hot-pressed alumina-SiC(w) composites, has been conducted. The results, shown in Table 1, indicate that devitrifying the glass phase or adding a reinforcing phase improves the mechanical properties of the alumina.

TABLE 1 COMPARISON OF THE STRENGTH AND TOUGHNESS OF MONOLITHIC ALUMINA AND ALUMINA MATRIX COMPOSITES

| MATERIAL | PROCESSING | FRACTURE TOUGHNESS | FLEXURAL STRENGTH |
|---|-----------------------------|------------------------------------|-------------------|
| Al ₂ O ₃ (10 v% glass) | sintered | ≈ 3 MPa · m ^{1/2} [5] | ≈ 300 MPa [5] |
| Al ₂ O ₃ (glass phase devitrified) | sintered and recrystallized | 4 - 5 MPa · m ^{1/2} [6] | ≈ 300 MPa [5],[7] |
| Al ₂ O ₃ /TiC (particulate) | hot-pressed | 3 - 6 MPa · m ^{1/2} [8] | 600 - 800 MPa [9] |
| Al ₂ O ₃ /SiC (20 v% whiskers) | hot-pressed | 8 - 10 MPa · m ^{1/2} [10] | 650 MPa [8] |
| Al ₂ O ₃ /SiC (30 v% platelets) | hot-pressed | 8 MPa · m ^{1/2} [4] | 150 - 350 MPa [4] |

Researchers have investigated the addition of various oxides as liquid phase sintering aids for this system. Tiegs and Becher^[11] have reported achieving 95% of theoretical density in 10 wt% SiC(w) composites using MgO and Y₂O₃ as sintering aids. These composites are reported to have a flexural strength of 330 MPa and fracture toughness of 7 MPa · m^{1/2}.

Initial investigations examined the microstructure and mechanical properties resulting from the addition of TiO₂ and MnO₂ as sintering aids in the alumina SiC(w) composite. These oxides have been used as liquid phase sintering aids for high purity alumina^{[12],[13],[14]}.

Hot-pressed samples of the composite with and without flux (oxides) were prepared by the Coors Ceramics Company. The mechanical properties they measured are shown in Table 2^[15]. The addition of the flux reduced the temperature required for sintering to high density which improved the flexural strength of the composites.

TABLE 2 MECHANICAL PROPERTIES OF HOT-PRESSED $\text{Al}_2\text{O}_3/10\text{wt}\% \text{SiC(w)}$ WITH THE ADDITION OF $\text{TiO}_2/\text{MnO}_2$ SINTERING AID

| | FRACTURE TOUGHNESS | FLEXURE STRENGTH | DENSITY |
|--------------|-------------------------------------|------------------|----------------------|
| WITH FLUX | 5 $\text{MPa} \cdot \text{m}^{1/2}$ | 450 MPa | 3.82 g/cm^2 |
| WITHOUT FLUX | 5 $\text{MPa} \cdot \text{m}^{1/2}$ | 240 MPa | 3.54 g/cm^2 |

Examination of the surface of the whiskers in these materials using a JOEL scanning electron microscope (SEM) showed evidence of extensive porosity and degradation due to chemical reaction between the SiC and the additives. Energy Dispersive Spectroscopy (EDS) conducted on the samples indicated that the manganese was present at the whisker surface, while the titania was found as disperse particles within the matrix. Transmission electron microscope (TEM) studies conducted by Popoola and Heuer^[16], on the alumina-SiC(w) composites, with and without flux, showed degradation due to the formation of an amorphous manganese rich phase at the whisker-matrix interface, triple-points and grain boundaries.

The evidence of whisker degradation creates a serious problem in ceramic composite systems. A single crystal of a ceramic material can be much stronger than many metals (ie. diamond) due to the ionic and covalent nature of the atomic bonds. However, the presence of flaws within the bulk material creates weak spots which cause these materials to fail catastrophically. Whiskers, fibers, or particulates are added to monolithic ceramic materials to increase their toughness. Figure 1 shows two methods by which these reinforcements are able to increase the toughness of the ceramic.

The first mechanism for increased toughness is the result of the reinforcement impeding crack growth by deflecting the crack path along the interface. The change in the crack propagation direction requires additional energy to allow continued crack growth. The second mechanism, pull-out, is initiated as the crack continues to propagate. Friction between the matrix and reinforcement resists the opening of the crack, so more energy is required for the crack to continue propagating. For either of these toughening mechanisms to operate successfully, the reinforcement/matrix interface must be weaker than the reinforcement and the surrounding matrix. Also, the reinforcement must be relatively flaw-free so that the crack can not propagate through it.

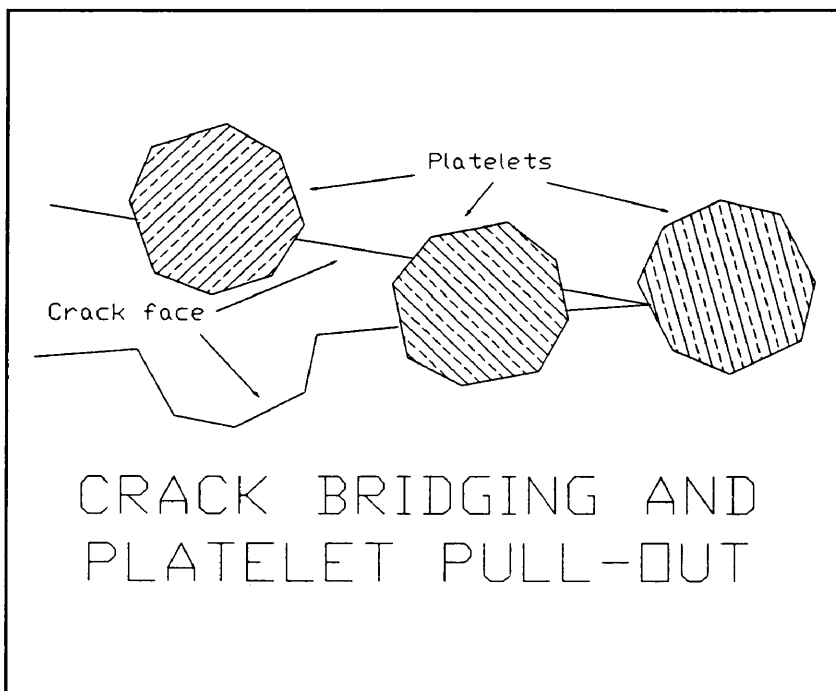
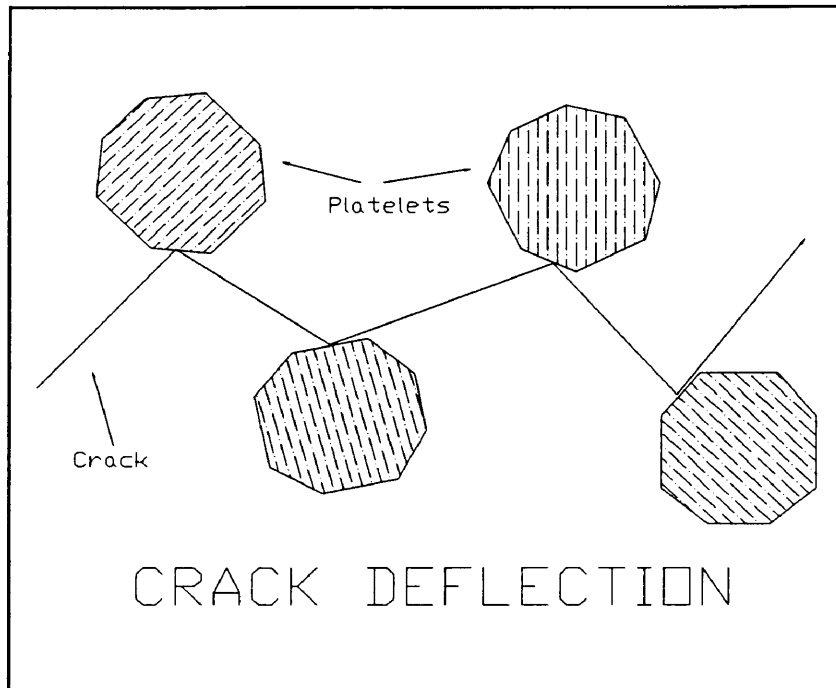


Figure 1 Crack deflection and retardation due to platelets within the matrix.

SEM examination found that the whiskers had reacted with the $\text{TiO}_2\text{-MnO}_2$ flux creating a reaction layer at the interface thus degrading the surface of the whisker (Figure 2). These conditions significantly reduce the effectiveness of the reinforcement as described previously. Since the whiskers reacted with the sintering aid, it was decided that the $\text{TiO}_2 - \text{MnO}_2$ sintering aid system would not be commercially viable.

This required the search for a different sintering aid. Since it is well known that a liquid phase helps in the sintering of high purity alumina^[3], investigation of a glass system which would not react with the SiC, but would aid in sintering the composite, commenced. In addition, a glass system that would easily devitrify for increased toughness, was desired. The investigation began with a study of the thermodynamics of the system to identify candidate materials. Glass compositions were selected and the resulting glasses were mixed with the SiC platelets to prepare model composite samples for microstructural examination. These studies then provided background for several families of liquid phase sintering aids for alumina-SiC composites.

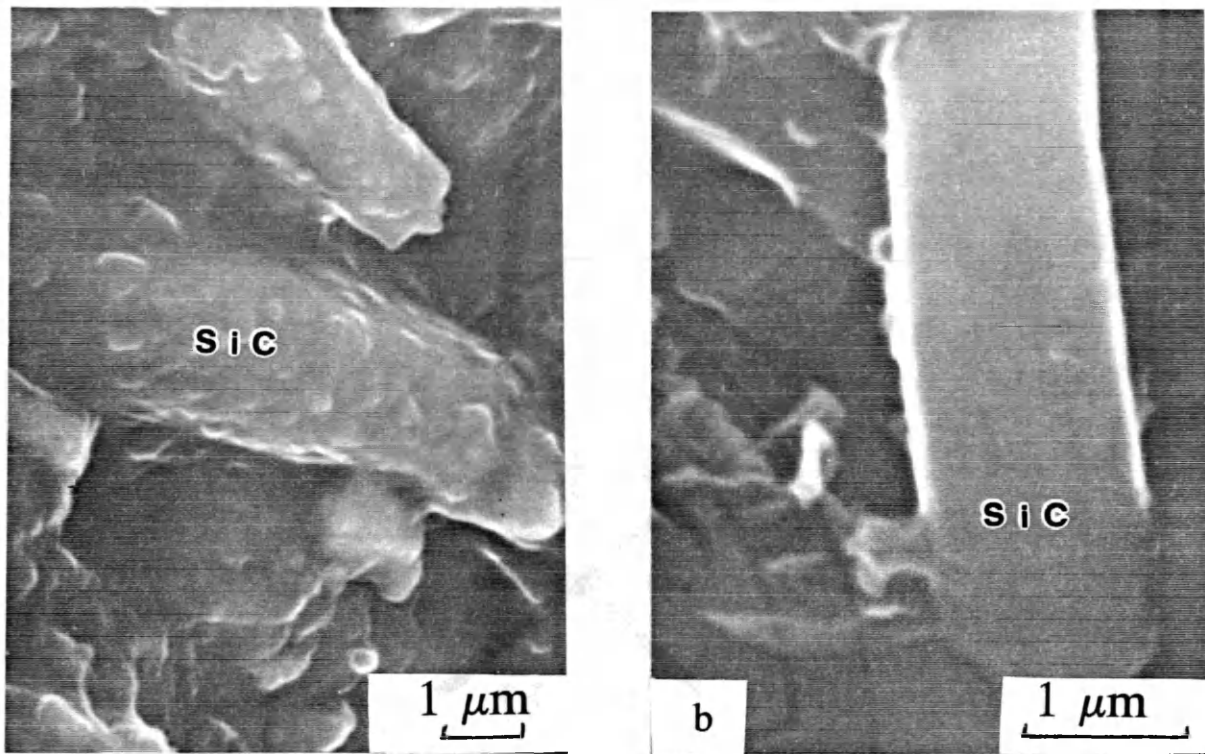


Figure 2 Surface of a SiC whisker in alumina a) with MnO₂-TiO₂ flux and b) without flux.

CHAPTER 2

SINTERING AID DEVELOPMENT

2.1 Sintering Aid Selection Criteria

The main criteria for the selection of sintering aids for the alumina/silicon carbide composite system is that the sintering aid not oxidize the silicon carbide reinforcement. Oxidation of the SiC weakens its reinforcement capability.

Another criteria for this system is that the sintering aid form a liquid phase during sintering to allow the sintering process to operate at a lower temperature and pressure. This criteria is met with the use of a glass-forming sintering aid. However, a residual glass phase in the composite will reduce the potential for high strength and fracture toughness at high temperature.

Therefore an additional requirement is placed on the potential sintering aid to be easily devitrified to increase both the high temperature and room temperature mechanical properties of the final composite. The sintering aid compositions selected for further study are lithia-alumina-silicate (LAS) and magnesia-alumina-silicate (MAS) glass-ceramics. These compositions are summarized in Table 3.

Table 3 SINTERING AID COMPOSITIONS

| COMPOSITION | LAS GLASS (wt%) | MAS GLASS (wt%) |
|--------------------------------|-----------------|-----------------|
| Al ₂ O ₃ | 20 | 30 |
| SiO ₂ | 70 | 45 |
| TiO ₂ | 5 | 10 |
| Li ₂ O | 5 | NA |
| MgO | NA | 15 |

These compositions were selected, based on thermodynamics, to have minimal reaction with SiC and form glass-ceramics with high melting points. Figure 3 and Figure 4 show the glass-ceramic forming region (shaded areas) of each of these compositions (excluding the TiO₂ nucleating agent)^{[17],[18],[19]}. Glass LAS is in the β -spodumene phase field and on the SiO₂ - β -spodumene solid solution phase boundary. Glass MAS is in the cordierite phase field and in the cordierite-forsterite-spinel composition triangle.

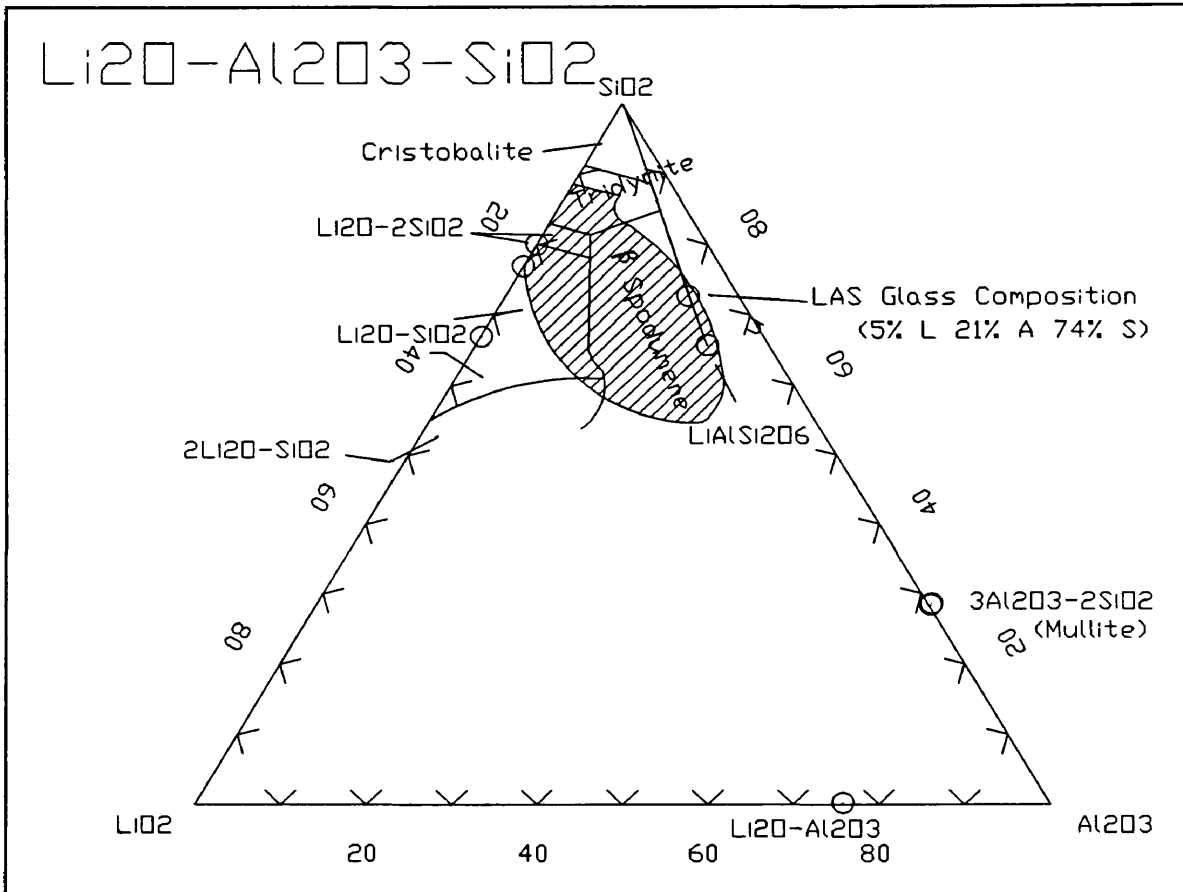


Figure 3 Ternary phase relationship of the LAS system^{[17],[18]}.

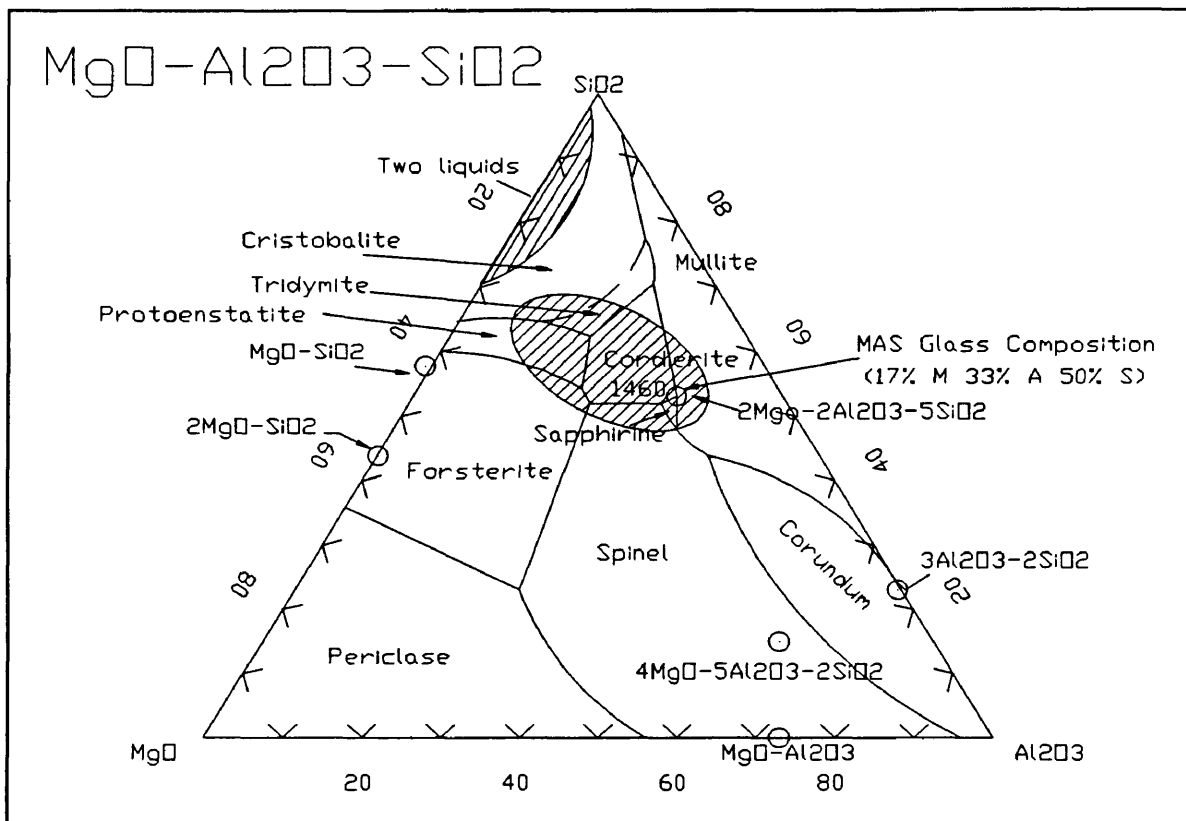


Figure 4 Ternary phase relationship of the MAS system^{[17],[19]}.

2.2 Glass Formation

Glasses are noncrystalline materials which have a gradual transition in viscosity from solid to liquid upon melting, unlike crystalline materials in which there is an abrupt change from solid to liquid, i.e., a melting point^[20] (Figure 5). Formation of oxide glass requires more than simply cooling a melt fast enough to prevent the formation of an ordered, crystalline solid. Zachariasen^[21] proposed that glasses have a random network structure, as shown in Figure 6, and that specific conditions must be met for an oxide to form a glass. The requirements for glass formation are:

- 1) an oxygen atom must not be linked to more than two cations,
- 2) the number of oxygen atoms surrounding the cation must be small,
- 3) the oxygen form polyhedra which can only share corners, not edges or faces,
- 4) at least three corners of the polyhedral should be shared (this condition may not always be required).

A glass composition may consist of network formers, intermediates and modifiers. The glass network formers, such as SiO_2 , GeO_2 , P_2O_5 , B_2O_3 and As_2O_5 , must meet the criterion proposed by Zachariasen. Intermediate oxides are those oxides which by themselves can not form a glass network, but can substitute for network formers in the structure of the glass. Examples of intermediate oxides are Al_2O_3 and BeO . The aluminum ion can be coordinated with four or six oxygen atoms forming tetrahedral and octahedral groups. The tetrahedral AlO_4 group can replace a SiO_4 group within the network. However, the difference in charge between the Si ion (+4) and the Al ion

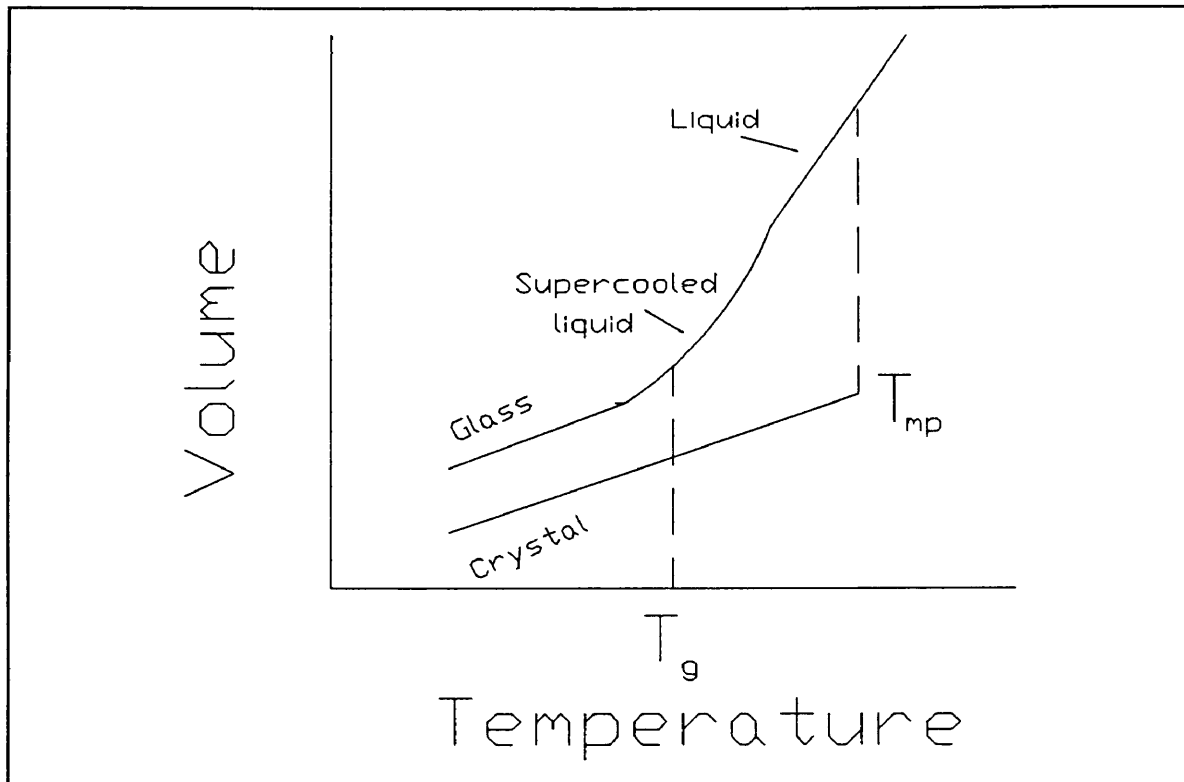


Figure 5 Volume-temperature relationships for glass and crystalline solids^[20].

(+3) will require an additional positive charge in the structure to provide electrical neutrality.

The additional positive charge is provided by the network modifiers. Alkali metals such as sodium, lithium and potassium provide charge neutrality by occupying the holes present within the network structure. The addition of modifiers to the glass can alter the glass properties, such as lowering the viscosity of the glass or increasing the thermal expansion coefficient.

The gross chemical formula for glasses can be represented by the formula: $A_m B_n O$, where B represents the glass-former elements plus the intermediate elements, and

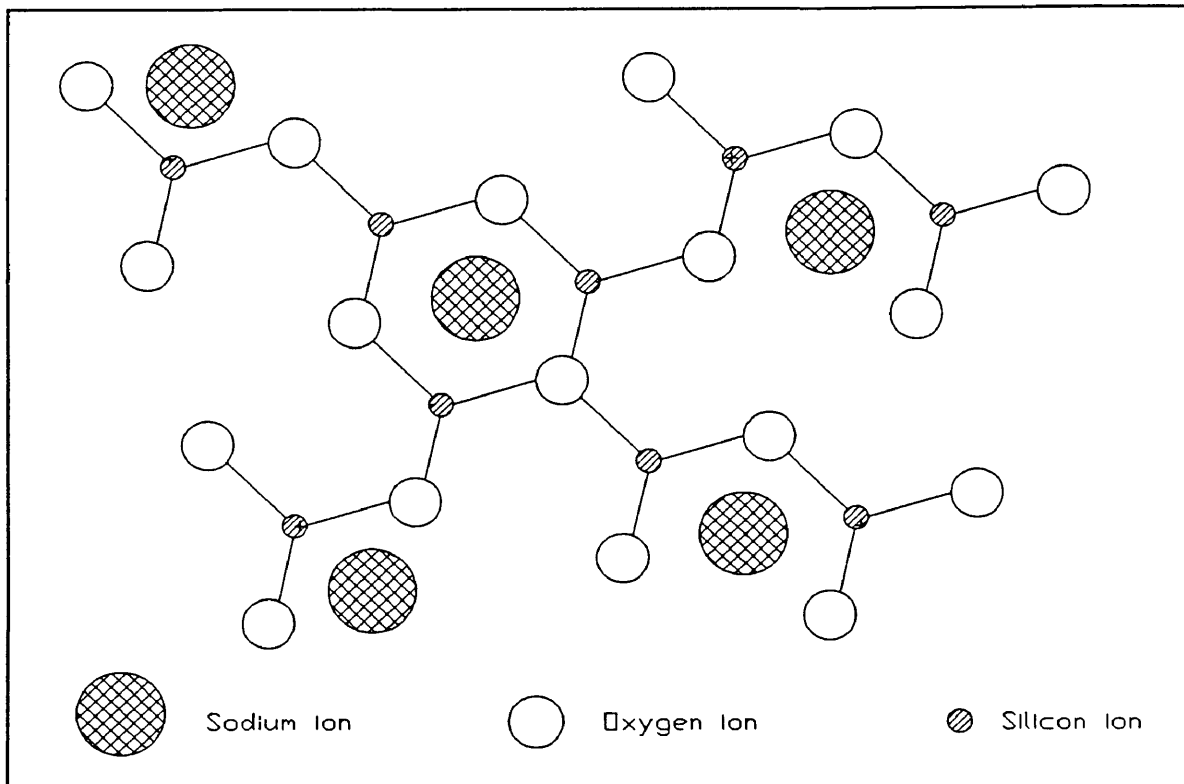


Figure 6 Representation of the random network structure of glass^[21].

A, the modifier elements. The subscripts m and n represent the number of A and B atoms per oxygen atom and need not be integers. To satisfy the criteria set forth by Zachariasen, the allowable range for n ($1/n$ is equivalent to the oxygen to network former ratio) is 0.4 to 0.5.

2.3 Glass Devitrification and Glass-Ceramics

All glasses are in an unstable form and will devitrify under the right conditions. Devitrification may not occur for many years, as in the case of sodium silicate glass, or may occur almost immediately, as in the case of a quenched amorphous phase metal.

A glass-ceramic is formed as liquid glass, then devitrified through controlled heat treatment, creating a microcrystalline solid. The devitrification is most easily accomplished through the addition of a nucleating agent. The nucleating agent provides sites for crystallite formation in the same manner that microscopic dust particles provide crystal growth nucleation sites in the ice/water system. It is important that the nucleating agent provide a large number of crystallization sites to attain a fine-grained microstructure. The nucleating agent will often be soluble in the glass, but on cooling, will either form a fine, disperse particulate or change the structure of the glass^[17]. Typical oxides used as nucleating agents in glass-ceramics include, TiO_2 , P_2O_5 , and V_2O_5 . The resulting glass-ceramic is much stronger and more heat resistant than the precursor glass.

Many ceramic materials, such as Al_2O_3 , Si_3N_4 , and SiC , contain small additions of other oxides to enhance their sinterability. These oxide additions tend to form a glass phase at the grain boundaries and triple points, resulting in poorer mechanical properties and lower the temperature at which the materials can be used. Several researchers have investigated the possibility of devitrifying the glass phase in alumina in situ^{[3],[6],[22]} to increase the fracture toughness and reduce creep at high temperatures. Both of these improvements were realized by devitrifying the glassy boundary phase.

2.4 Thermodynamic Analysis of Sintering Aids

Individual Oxides

Effective sintering aids for the alumina-SiC system should have minimal reaction with the silicon carbide. In Figure 7 the various oxidation reactions of SiC and the temperature dependence of their standard free energies (ΔG°) are shown^{[23],[24]}. In the temperature range chosen for sintering, 1300 - 1500°C (1600 - 1800°K), the most likely oxidation reaction for the SiC will be:



shown as equation 1 on Figure 7.

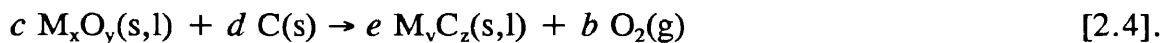
The important reactions of the individual metal oxides will be:

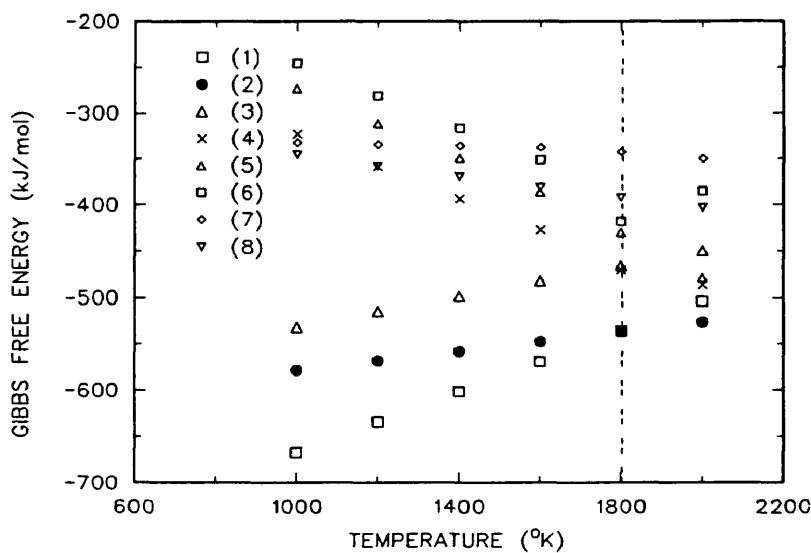


and



adding the reverse of [2.2] to [2.3] gives:





- (1) $\text{SiC(s)} + \text{O}_2(\text{g}) = \text{SiO}_2(\text{qu}) + \text{C(s)}$
- (2) $\frac{2}{3} \text{SiC(s)} + \text{O}_2(\text{g}) = \frac{2}{3} \text{SiO}_2(\text{qu}) + \frac{2}{3} \text{CO(g)}$
- (3) $\frac{1}{2} \text{SiC(s)} + \text{O}_2(\text{g}) = \frac{1}{2} \text{SiO}_2(\text{qu}) + \frac{1}{2} \text{CO}_2(\text{g})$
- (4) $\text{SiC(s)} + \text{O}_2(\text{g}) = \text{SiO(g)} + \text{CO(g)}$
- (5) $2 \text{SiC(s)} + \text{O}_2(\text{g}) = 2 \text{Si(s)} + 2 \text{CO(g)}$
- (6) $2 \text{SiC(s)} + \text{O}_2(\text{g}) = 2 \text{SiO(g)} + 2 \text{C(s)}$
- (7) $\text{SiC(s)} + \text{O}_2(\text{g}) = \text{Si(s)} + \text{CO}_2(\text{g})$
- (8) $\frac{2}{3} \text{SiC(s)} + \text{O}_2(\text{g}) = \frac{2}{3} \text{SiO(g)} + \frac{2}{3} \text{CO}_2(\text{g})$

Figure 7 Temperature dependence of ΔG° for oxidation reactions of $\text{SiC}^{[23], [24]}$. Note that the dominant reaction changes at 1800°K.

Combining reaction [2.1] with reaction [2.4] and [2.1] with the reverse of [2.2] results in the following relationships for the reaction of SiC with individual oxides:



and



In reactions [2.2] through [2.6] the coefficients represented by the italic letters are chosen so that the equations are balanced. The standard free energies of reactions [2.5] and [2.6] are respectively,

$$\Delta G^\circ_5 = \Delta G^\circ_1 + \Delta G^\circ_4 = \Delta G^\circ_1 + \Delta G^\circ_3 - \Delta G^\circ_2$$

and

$$\Delta G^\circ_6 = \Delta G^\circ_1 - \Delta G^\circ_2.$$

For a reaction to occur, the Gibbs free energy (ΔG°) of the reaction must be less than zero. Therefore, an oxide will not react with the SiC if the free energy of the reaction is positive. For the oxides studied, ΔG°_1 and ΔG°_2 have values less than zero while ΔG°_4 has values greater than zero. These values can be found in Appendix A. In this case, reactions [5] and [6] will not proceed when ΔG°_5 and ΔG°_6 have positive values, which occurs when $\Delta G^\circ_1 > \Delta G^\circ_2$ and $(-\Delta G^\circ_4)$. The free energy values for

various oxides were obtained for reactions [2.2] and [2.4] in the sintering temperature range to identify candidate materials for the formulation of the glass sintering aid. A plot of the ΔG°_2 versus $(-\Delta G^\circ_4)$ values (Figure 8) indicates which oxides will and will not react with the SiC. The oxides which will not react are those with free energies lower than the free energy of silica, and are found in the lower left quadrant of Figure 8. Oxides of elements in any of the other quadrants may react with silicon carbide if the reaction kinetics are favorable. Details of these calculations are contained in Appendix A.

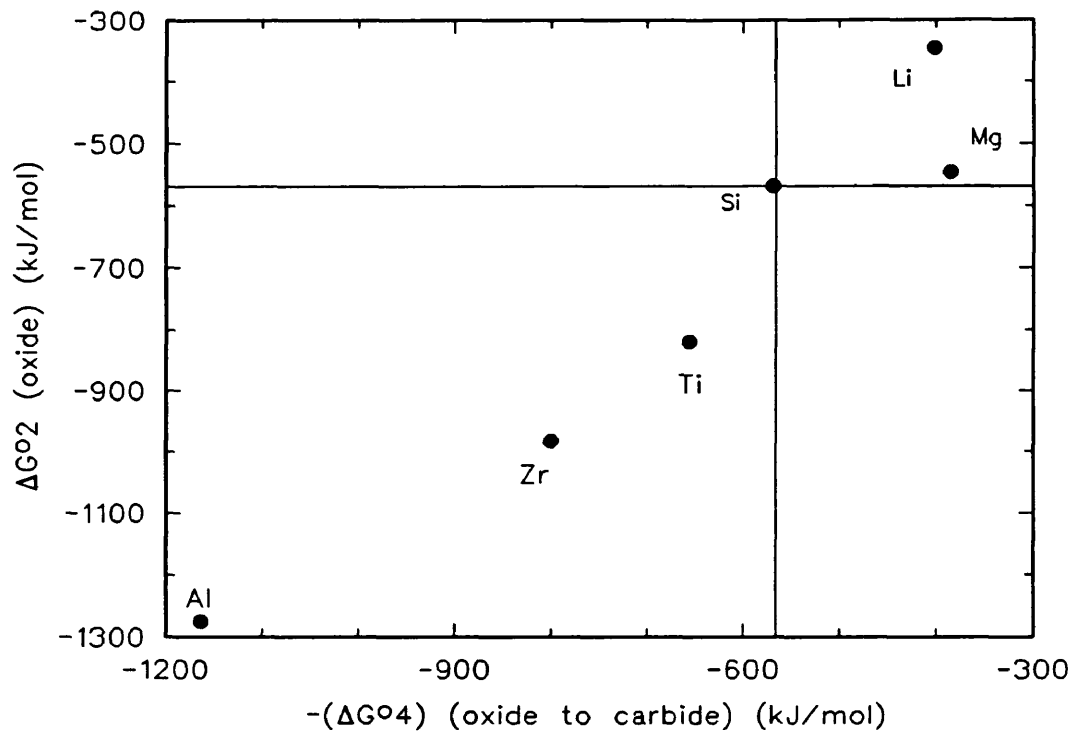


Figure 8 Relationship between ΔG° of the reaction of various oxides with SiC at 1600°C (1800°K)^[23,24]. Oxides of elements in the lower left quadrant will not react with SiC to form the metal carbide because they have a lower free energy than the for the formation of SiC from SiO_2 .

Oxide Systems

The program SOLGASMIX^[25] was used to model the global equilibrium thermodynamics of the composites. In the previous section, the thermodynamic calculations were based on one component reacting only with SiC. In SOLGASMIX, the thermodynamic calculations include all of the components in the system and their reactions with each other, not just the SiC. SOLGASMIX uses the equation

$$(G/RT) = \sum n_i[(g^\circ/RT)_i + \ln a_i]$$

to minimize the system free energy with respect to n_i for constant temperature and pressure values. Input required by SOLGASMIX for the free energy minimization calculations includes the number, composition and quantity of each phase present, the temperature of interest, and the Gibbs free energy of formation from the reference state for each component.

The initial and calculated equilibrium moles of each phase present in each composite are shown in Table 4.

TABLE 4 THERMODYNAMIC MODEL OF ALUMINA/SiC COMPOSITES AT 1800°K USING "SOLGASMIX"

| PHASE | INITIAL MOLES IN ASTM | EQUILIB. MOLES IN ASTM | INITIAL MOLES IN ASL | EQUILIB. MOLES IN ASL | INITIAL MOLES IN ASM | EQUILIB. MOLES IN ASM |
|------------------------------------|-----------------------------|------------------------------|----------------------------|-----------------------------|----------------------------|-----------------------------|
| SiO (g) | 0 | 0 | 0 | 0 | 0 | 0 |
| CO ₂ (g) | 0 | 0 | 0 | 0 | 0 | 0 |
| CO (g) | 0 | 0.006 | 0 | 0 | 0 | 0.001 |
| O ₂ (g) | 0 | 0 | 0 | 0 | 0 | 0 |
| Si (l) | 0 | 0 | 0 | 0.025 | 0 | 0 |
| SiO ₂ (s) | 0 | 0.075 | 0.058 | 0.054 | 0.037 | 0.057 |
| Al ₂ O ₃ (s) | 1.270 | 1.270 | 1.388 | 1.388 | 1.396 | 1.377 |
| Al ₄ C ₃ (s) | 0 | 0 | 0 | 0 | 0 | 0 |
| TiO ₂ (s) | 0.050 | 0 | 0.003 | 0 | 0.063 | 0 |
| TiC (s) | 0 | 0.050 | 0 | 0.003 | 0 | 0.063 |
| SiC (s) | 0.250 | 0.175 | 0.250 | 0.230 | 0.250 | 0.184 |
| C (s) | 0 | 0 | 0 | 0 | 0 | 0.002 |

continued

| PHASE | INITIAL MOLES IN ASTM | EQUILIB. MOLES IN ASTM | INITIAL MOLES IN ASL | EQUILIB. MOLES IN ASL | INITIAL MOLES IN ASM | EQUILIB. MOLES IN ASM |
|------------------------------------|-----------------------|------------------------|----------------------|-----------------------|----------------------|-----------------------|
| Mn (s) | 0.056 | 0 | NA | NA | NA | NA |
| Mn ₃ C (s) | 0 | 0.019 | NA | NA | NA | NA |
| Li ₂ O (s) | NA | NA | 0.008 | 0 | NA | NA |
| Li ₂ C ₂ (s) | NA | NA | 0 | 0.008 | NA | NA |
| SPODUMENE (s) | NA | NA | 0 | 0 | NA | NA |
| MgO (s) | NA | NA | NA | NA | 0.019 | 0 |
| MgC ₂ (s) | NA | NA | NA | NA | 0 | 0 |
| FORSTERITE (s) | NA | NA | NA | NA | 0 | 0 |
| SPINEL (s) | NA | NA | NA | NA | 0 | 0 |
| CORDIERITE (s) | NA | NA | NA | NA | 0 | 0.009 |

These values are based on 100 grams of composite with the following compositions:

Table 5 COMPOSITE COMPOSTIONS

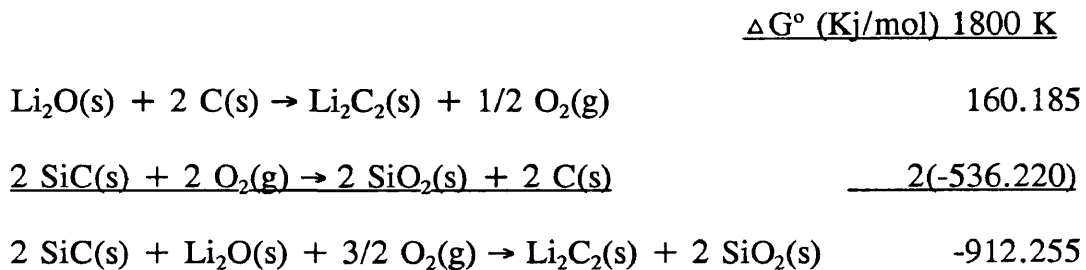
| COMPOSITE | Al ₂ O ₃ (wt%) | SiC (wt%) | Sintering Aid (wt%) | | | | | |
|-----------|---|--------------|--------------------------------|------------------|------------------|-------------------|-----|------------------|
| | | | Al ₂ O ₃ | SiO ₂ | TiO ₂ | Li ₂ O | MgO | MnO ₂ |
| ASTM | 76 | 16 | 8 | | | | | |
| | | | | | 50 | | | 50 |
| ASL | 85 | 10 | 5 | | | | | |
| | | | 20 | 70 | 5 | 5 | | |
| ASM | 85 | 10 | 5 | | | | | |
| | | | 30 | 45 | 10 | | 15 | |

At equilibrium < 50% of SiC will remain in the composite when a TiO₂ and MnO₂ flux is present. However, with the LAS and MAS glass sintering aids > 90% and > 75%, respectively, of the SiC will remain at equilibrium for reactions at 1800°K. In all three cases, the model predicted the conversion of TiO₂ to TiC, which was not observed experimentally.

2.5 Glass Ceramic Sintering Aid

Alumina-silicate based glasses are promising candidates for use as sintering aids because alumina is already known to be nonreactive with the SiC. For the oxidation of SiC to occur, gaseous oxygen, in excess of the particle surface concentrations, must diffuse into the composite.

One candidate glass composition selected for further study in this project was a lithium-aluminum-silicate (LAS) glass-ceramic. Thermodynamically, the lithium oxide may react with the SiC platelets since the ΔG° of the formation of Li_2C_2 from Li_2O is slightly positive with respect to the formation of SiO_2 from SiC, as shown in Figure 8.

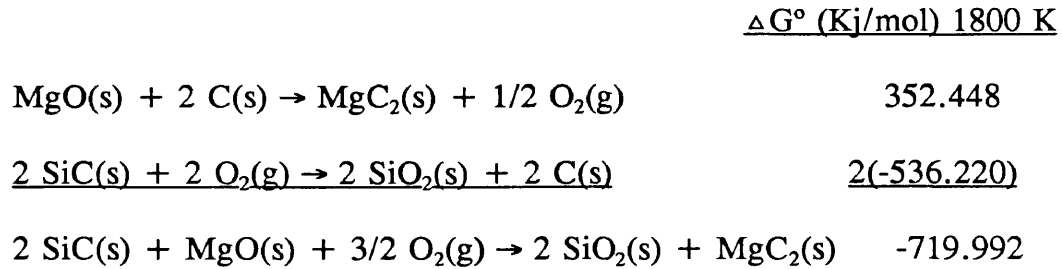


However, the LAS system has been used as a successful matrix material in composites with SiC fibers^[26]. The kinetics of the reaction may be the limiting factor in the prevention of SiC degradation.

The ability to devitrify the glass phase to form a glass ceramic improves the mechanical properties of the composite because the crystallites produced help deflect cracks, and a crystallized material is usually stronger than a glass phase at high temperatures.

Extensive research has been conducted on the LAS glass-ceramic reinforced with SiC fibers^[26]. These composites often have Nb₂O₅ added to assist in the devitrification of the glass to produce the glass-ceramic. Several researchers have identified layers of amorphous carbon and NbC surrounding the fibers in the toughest LAS-SiC composites^{[27],[28],[29],[30]}. It is believed that the brittle carbide layer allows interfacial debonding which results in easier crack deflection and fiber pullout from the matrix - thus increasing the composite toughness. However, in composite containing SiC platelets or whiskers, the formation of NbC will destroy the reinforcing capability of the SiC, so a different nucleating agent was required. Titania (TiO₂) is another common nucleating agent in glass-ceramics^[17]. According to the information on the standard free energy of formation of TiC, shown in Figure 8, TiO₂ should not react with SiC. However, the global thermodynamic modelling of the composite systems, using SOLGASMIX, predicted the TiO₂ would form TiC. Electron microscopy and EDS studies performed on the Al₂O₃/SiC composite with TiO₂ and MnO₂ additions (provided by the Coors Ceramics Company), located the TiO₂ only in the matrix as discrete particles, and not within the glassy interface of the whiskers and matrix. Therefore, TiO₂ was selected as the nucleating agent for our glass-ceramic sintering aid.

The other glass-ceramic composition chosen for further investigated was the magnesia-alumina-silicate (MAS) system. The magnesium, as shown in Figure 8, may react with the SiC, but as with the LAS glass-ceramic, the kinetics of the reaction should prevent degradation of the SiC reinforcement at the temperatures of interest.



A literature survey found very little published information on cordierite glass-ceramics reinforced with SiC. Corning Glass Works was granted a patent in 1988 on the manufacture of a cordierite/SiC(w) composite ^[28]. As with LAS, TiO₂ is the chosen nucleating agent for the MAS glass-ceramic system ^[20,28] for the reasons presented in the discussion of LAS.

CHAPTER 3

EXPERIMENTAL PROCEDURE

3.1 Composite Preparation

Composites were prepared by mixing alumina*, SiC platelets** and glass frit***, having the compositions shown in Table 3. Table 6 lists the composites prepared and the processing conditions for each.

Glass/SiC composites were prepared using a 10 wt% loading of the platelets to ensure no reaction would occur between the glass and silicon carbide at or above the devitrification temperature. The devitrification temperature was determined by differential thermal analysis (DTA). Each glass/SiC composite was cold pressed at 70 MPa (10,000 psi) in a hydraulic press****. Sintering of the glass and SiC was accomplished by heating the composites from 30°C to 935°C over 1.5 hours under flowing N₂, then they were held at 935°C for 45 minutes and cooled to 100°C over 2 hours in a Lindberg tube furnace.

* Grade RC-HP, Reynolds Chemicals, Richmond, VA.

** C-Axis (Alcan International Limiteé), Jonquieré, Québec, Canada.

*** Ferro Corporation, Cleveland, Ohio.

**** Fred Carver, Menomonee Falls, Wisconsin.

Each sintered glass/SiC sample was examined in the SEM* to detect evidence of a chemical reaction between the glass and the platelets.

Table 6 EXPERIMENTAL COMPOSITIONS AND PROCESS CONDITIONS

| COMPOSITE | TEMPERATURE | ATMOSPHERE | PRESSURE |
|-------------------|-------------|------------|---------------------|
| Glass/SiC | 1000 | Nitrogen | Atmospheric |
| Alumina/SiC/Glass | 1000 | Nitrogen | Atmospheric |
| Alumina/SiC/Glass | 1400 | Argon | Atmospheric |
| Alumina/SiC/Glass | 1500 | Argon | Atmospheric |
| Alumina/SiC/Glass | 1600 | Vacuum | Atmospheric |
| Alumina/SiC/Glass | 1600 | Vacuum | 70 MPa (10,000 psi) |
| Alumina/SiC | 1600 | Vacuum | 70 MPa (10,000 psi) |

X-ray diffraction** (copper $K\alpha$ radiation, $\lambda=1.541\text{\AA}$) was used to observe the extent of crystallization and to identify the crystallization products.

Eighty five wt% alumina, 10 wt% SiC platelets and 5 wt% glass frit were combined together with a small amount of distilled water and mixed for ~15 minutes. Then they were cold pressed in a hydraulic press at 70 MPa (10,000 psi) to form the

*JOEL JXA 840

** Rigaku Theta-2 Theta Diffractometer.

green composites. The green composites were sintered at 1000°C in a stagnant N₂ atmosphere, and at 1400°C and 1500°C in a stagnant argon atmosphere for 1 hour in a Lindburg tube furnace. No additional heat treatments were required to devitrify the glass phase. Their densities were measured, then they were analyzed by X-ray diffraction and by EDS in the SEM.

Eighty five wt% alumina, 10 wt% SiC platelets and 5 wt% glass frit were mixed together and placed in the inductively heated hot-press package and vacuum sintered without pressure at 1600°C. Figure 9 shows a photograph and a schematic of the hot-press and furnace assembly. Details on the design of the hot-press are described by Lewis^[31]. The powders were cold-pressed to 70 MPA (10,000 psi) inside of the furnace package before heating. The furnace was evacuated to <20 mT before power was applied to the inductance coil. The power was initially set to 5 kW and gradually raised to 6.5 kW as the temperature increased over a 30 minute period. After heating for 30 minutes the power was turned off and the furnace cooled under vacuum to room temperature. A tungsten-5% rhenium/tungsten-26% rhenium thermocouple was placed into the graphite die inside the furnace to measure the temperature near the composites.

A second set of composite powders was hot-pressed to 70 MPa (10,000 psi) at 1600°C for 30 minutes. The furnace was inductively heated over a 30 minute period before pressure was applied. The pressure and temperature were held constant for 30 minutes then the power was turned off and the furnace cooled under vacuum to room temperature. A tungsten-5% rhenium/tungsten-26% rhenium thermocouple was placed into the graphite die inside the furnace to measure the temperature near the composites.

An alumina/SiC composite was also hot-pressed. This composite contained 90 wt% Al₂O₃ and 10 wt% SiC. It was processed under the same conditions as the alumina/SiC/glass composites.

The density of each composite was determined by the Archimedes buoyancy method. Details on the calculation of the percent of theoretical density of the composites and Archimedes buoyancy equations are available in Appendix A.

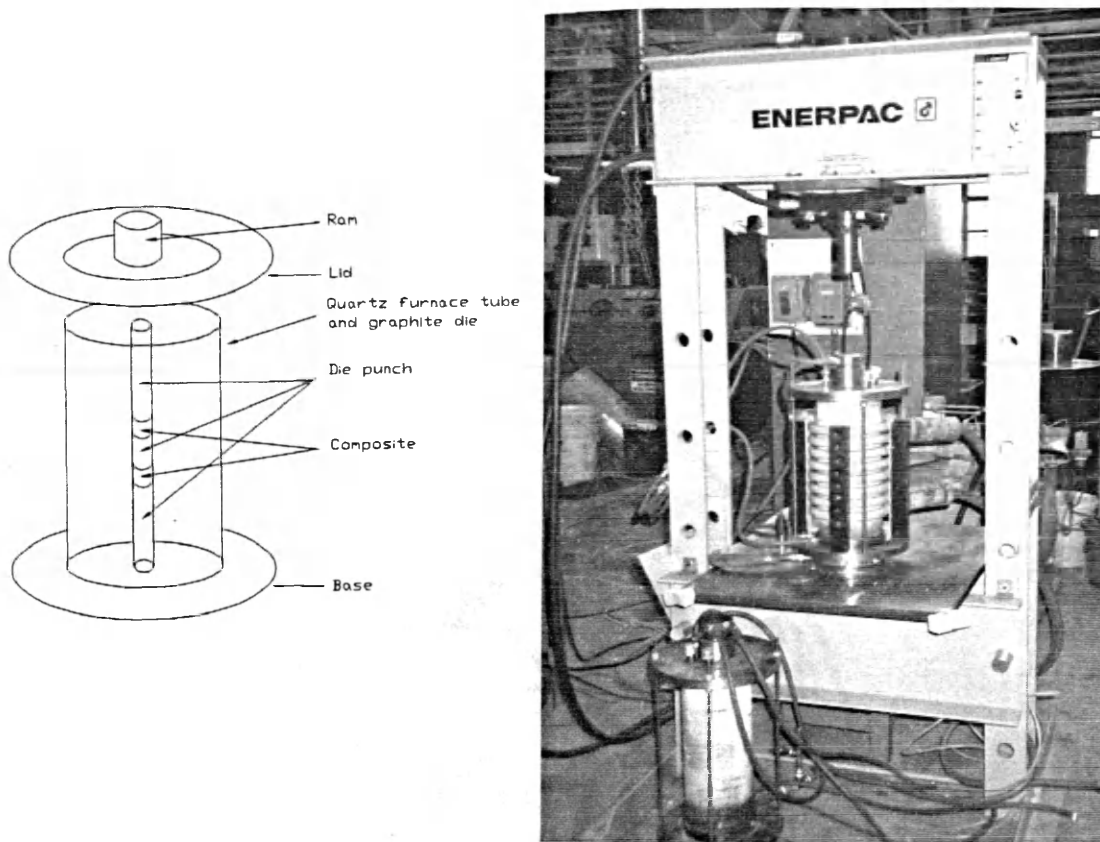


Figure 9 Schematic (left) and photograph (right) of the hot-press and furnace assembly.

3.2 Composite Microstructural Evaluation

Samples of composites sintered at 1000°C were ground using a quartz mortar and pestle to prepare them for x-ray diffraction. The composites sintered at 1600°C were too hard to grind, so solid pieces of each composite were analyzed by x-ray diffraction.

For examination under the SEM, pieces of each composite were either fractured from the sample or cut off using a diamond blade in a sectioning saw*. The composite pieces were each mounted on carbon stubs with carbon paint, then sputter coated with carbon to prevent charging of the sample by the electron beam.

* Mark V CS600-A, Mark V Laboratory, East Granby, CT.

CHAPTER 4

RESULTS AND DISCUSSION

4.1 Glass-Ceramic Processing Evaluation

Differential thermal analysis (DTA) was performed by the Coors Analytical Laboratory on the glass frits to determine the softening point and devitrification temperature of the glass. This information was used to determine whether a liquid phase would form during sintering of the composites and whether additional heat treatment would be required to devitrify any residual glassy phase present in the composite. The DTA results are shown in Figures 10 and 11.

4.2 Alumina/SiC Composite Microstructural Evaluation

The SEM micrographs in Figure 2, Chapter 1, show the surface of a SiC whisker in composites, prepared by Coors Ceramics Company, with and without the $\text{TiO}_2\text{-MnO}_2$ flux. The whiskers reacted with the flux creating a reaction layer at the interface, degrading the surface of the whisker. Both of these conditions significantly reduced the effectiveness of the reinforcement as described in Chapter 1.

In Figure 12, the as-received SiC platelets can be seen to have a sharp defined hexagonal structure. The aspect ratio is ≈ 10 . The average particle size is 16μ .

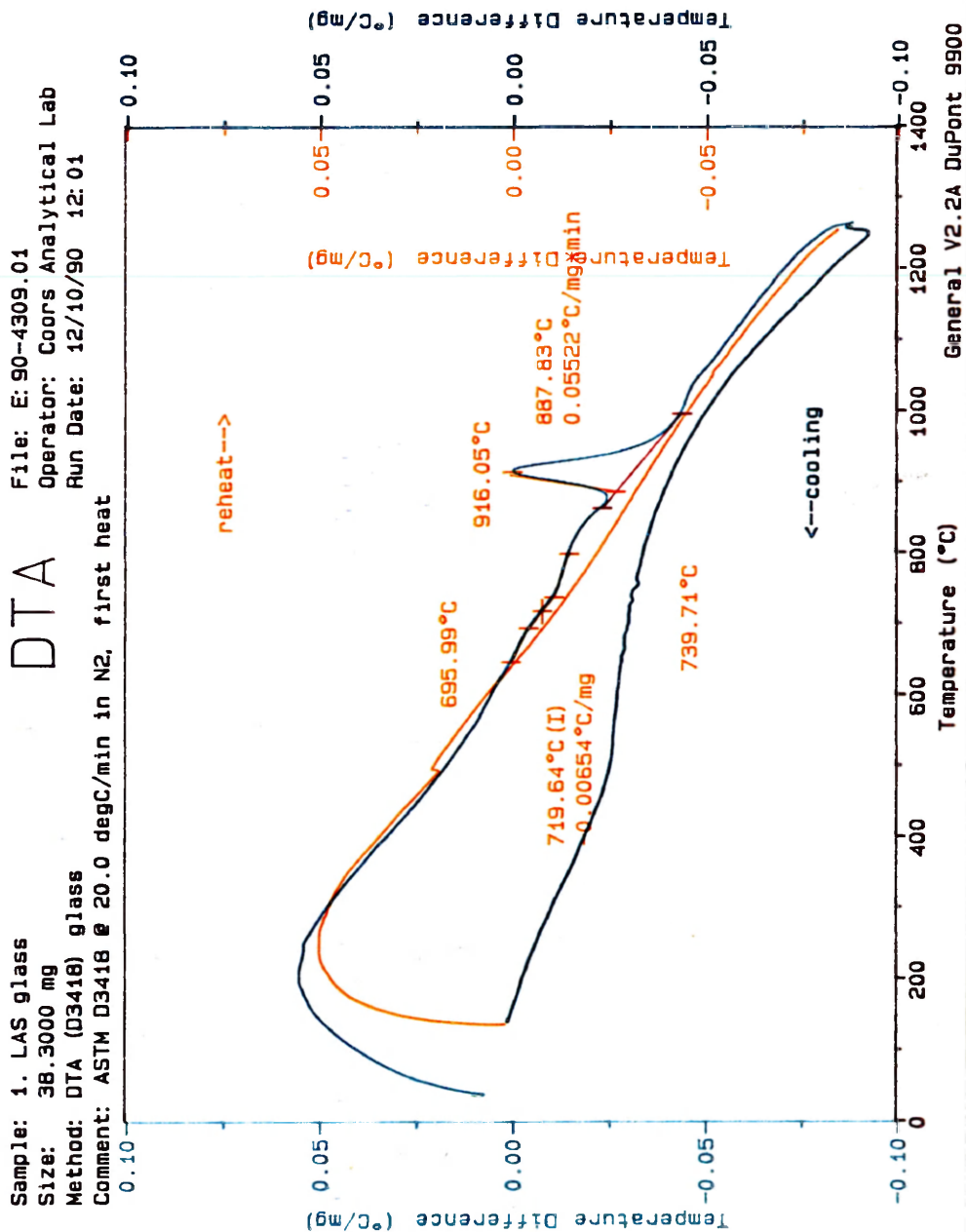


Figure 10 Differential thermal analysis of LAS glass frit.

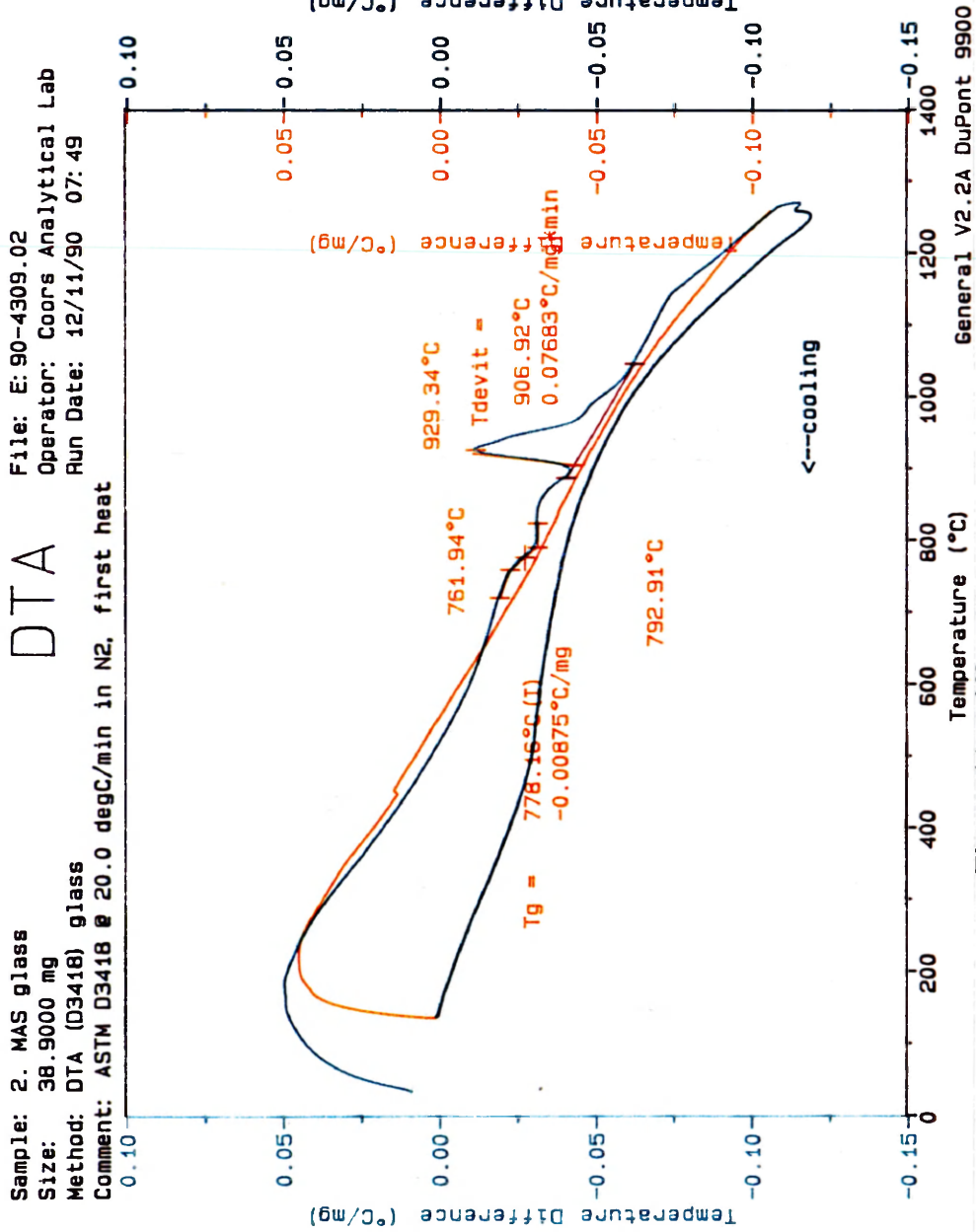


Figure 11 Differential thermal analysis of MAS glass frit.

General V2.2A DuPont 9900

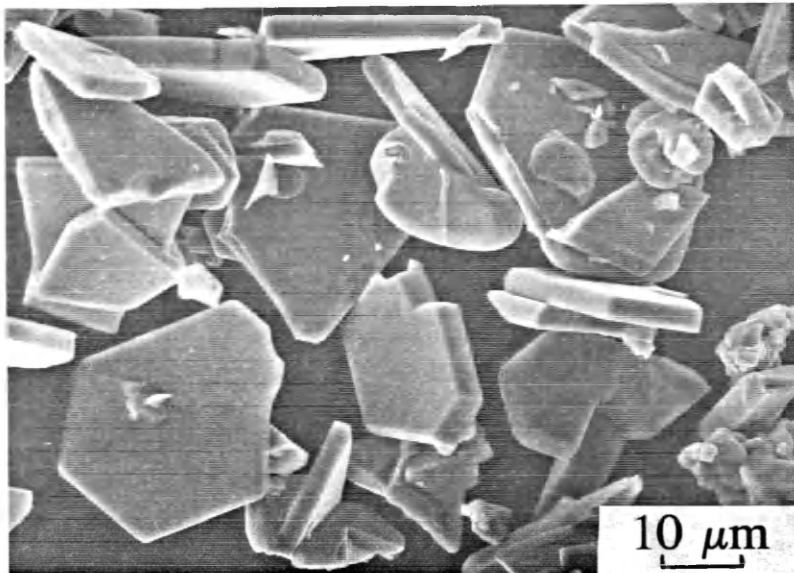


Figure 12 Typical SiC platelets.

After sintering the SiC platelets with each of the glass frits at 1000°C in flowing N₂, the composites were observed by SEM (Figure 13). The platelets still retain the sharp edges of their original condition, showing that no degradation has occurred.

The alumina/SiC/glass composites were then sintered at 1000°C, 1400°C, 1500°C and 1600°C. In all cases there did not appear to be any reaction between the SiC and the glass sintering aid (Figures 14, 15, 16, 17).

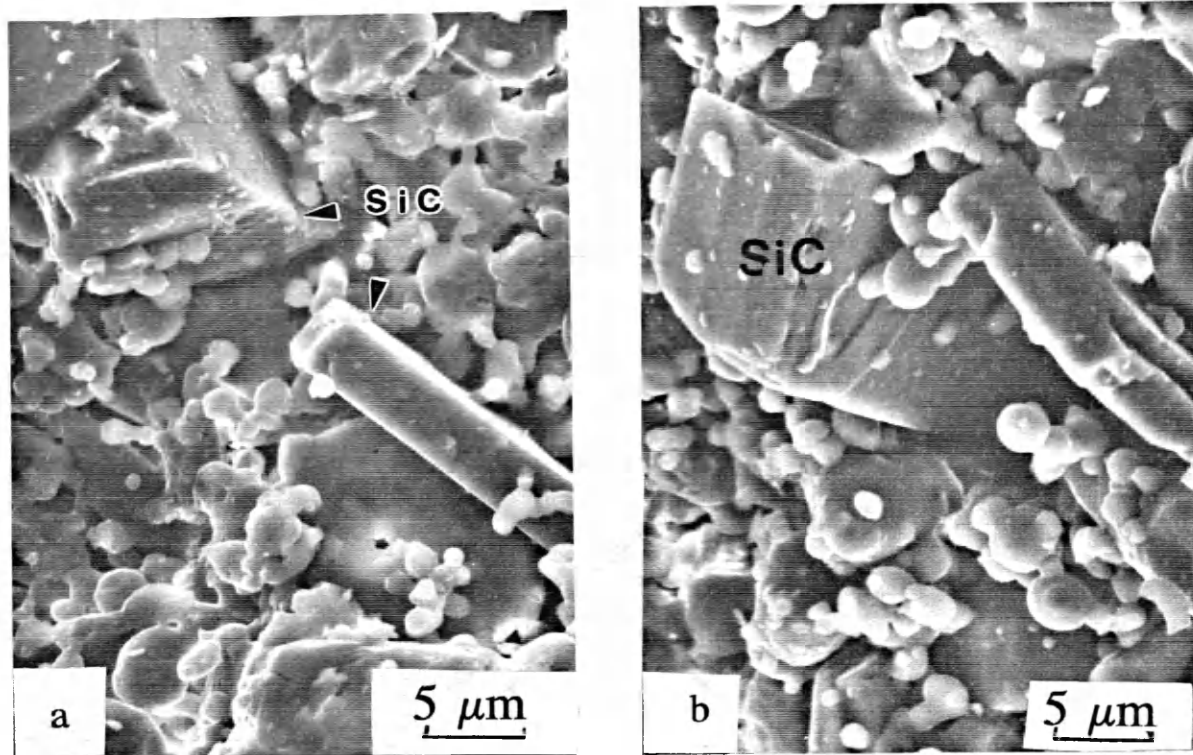


Figure 13 a) LAS and b) MAS glass sintered with 10 wt% SiC at 1000°C in N₂.

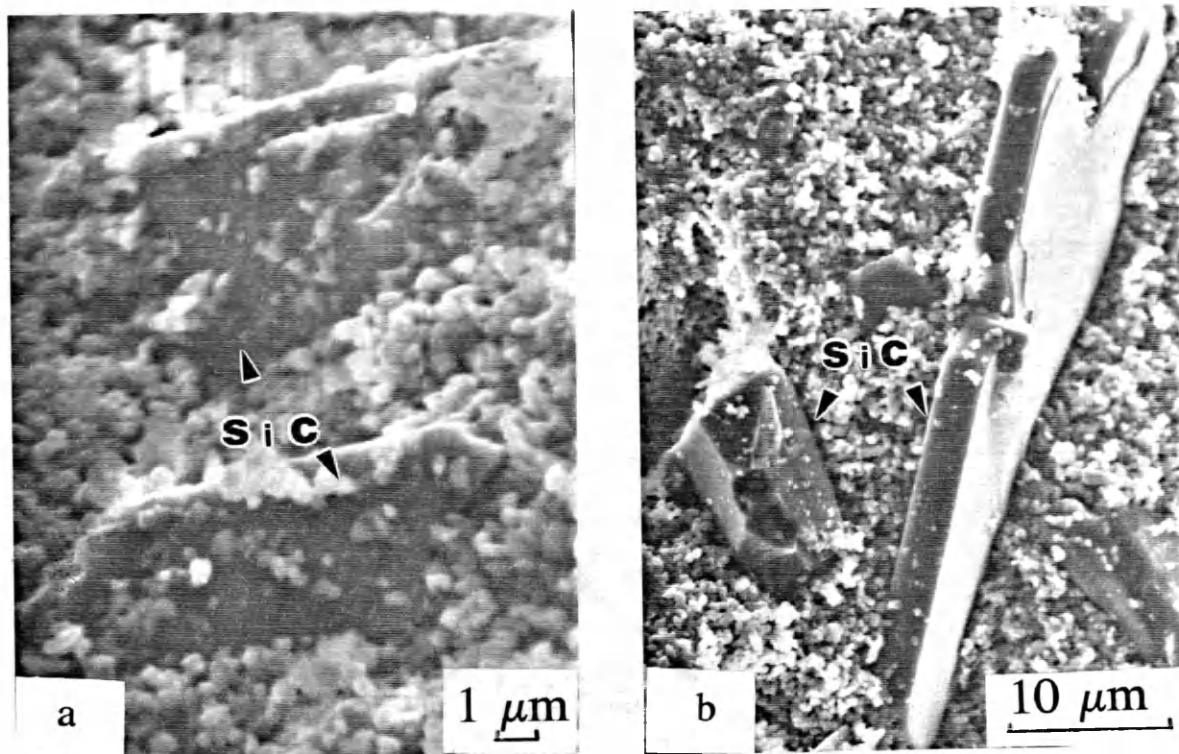


Figure 14 85 wt% alumina - 10 wt% SiC - 5 wt% a) LAS and b) MAS sintered at 1000°C in N₂.

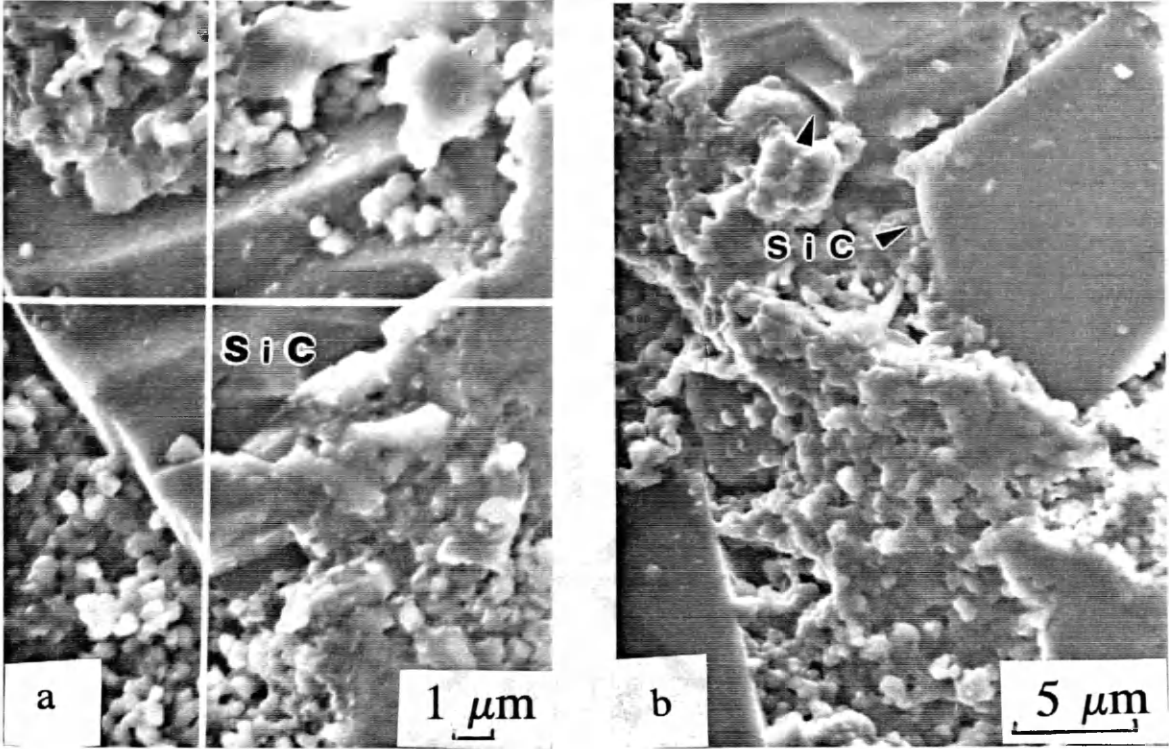


Figure 15 85 wt% alumina - 10 wt% SiC - 5 wt% a) LAS and b) MAS sintered at 1400°C in Ar.

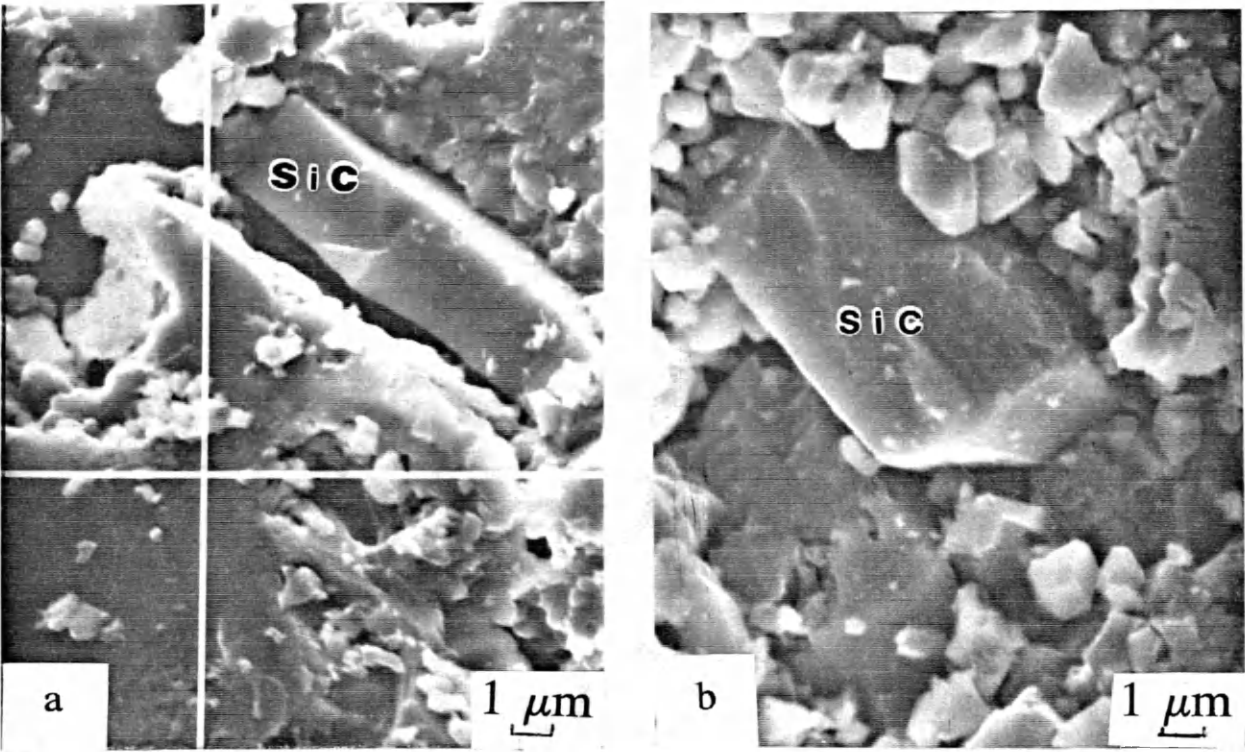


Figure 16 85 wt% alumina - 10 wt% SiC - 5 wt% a) LAS and b) MAS sintered at 1500°C in Ar.

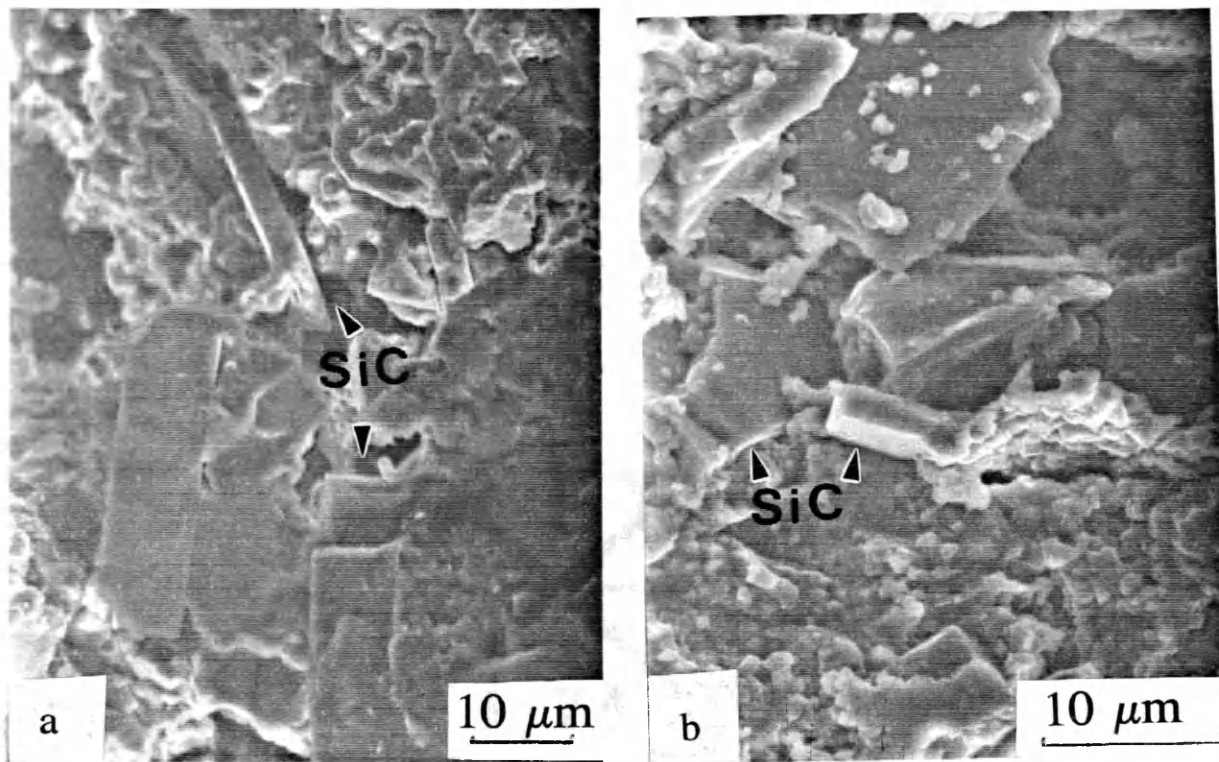


Figure 17 85 wt% alumina - 10 wt% SiC - 5 wt% a) LAS and b) MAS sintered at 1600°C in vacuum.

Alumina/SiC/glass and alumina/SiC composites were then sintered and hot-pressed at 1600°C and 70 MPa (10,000 psi). No evidence of reaction between the SiC and the glass sintering aid was found (Figures 18, 19, respectively). The amount of porosity in the hot-pressed composites with the sintering aid appears to be small and dispersed. The alumina/SiC without a sintering aid had larger pores concentrated around the platelets.

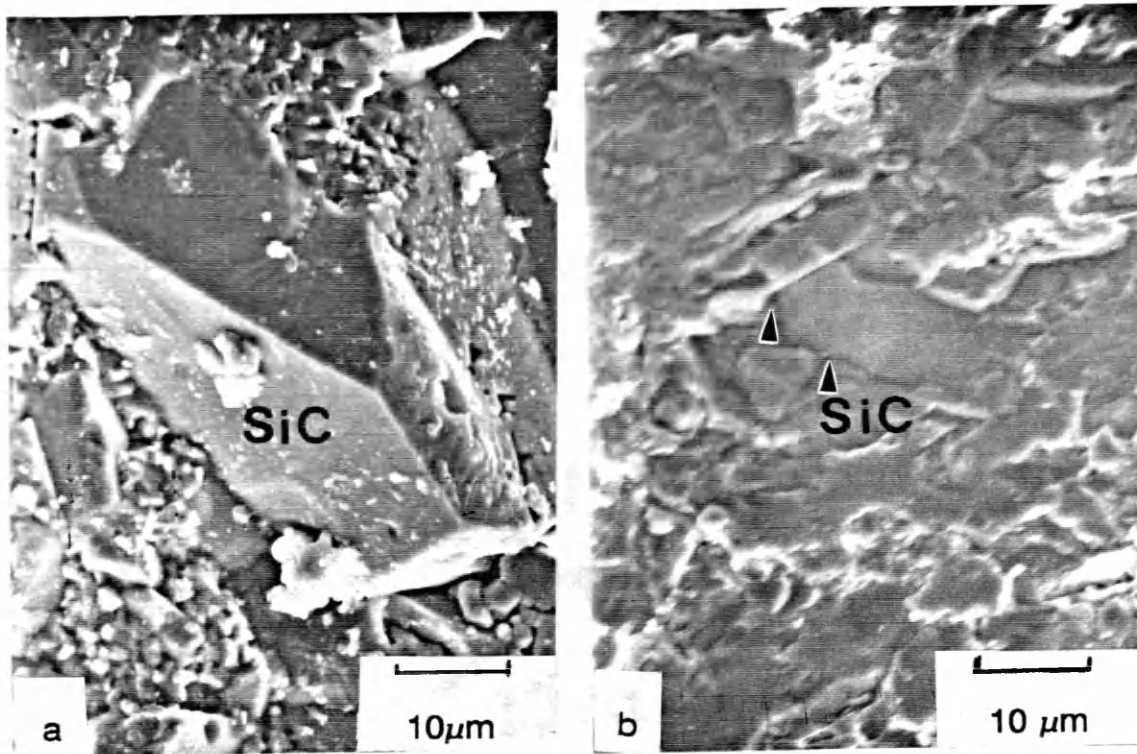


Figure 18 85 wt% alumina - 10 wt% SiC - 5 wt% a) LAS and b) MAS sintered and hot-pressed at 1600°C and 70 MPa (10,000 psi) in vacuum.

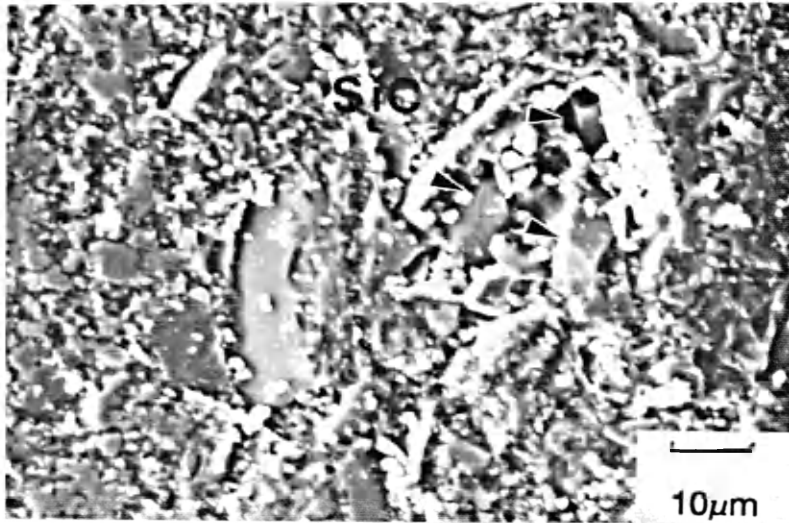


Figure 19 90 wt% alumina - 10 wt% SiC
sintered and hot-pressed at 1600°C and 70 MPa (10,000 psi) in vacuum.

4.3 X-Ray Diffraction of Alumina/SiC/Glass

X-ray diffraction analysis was performed on ground samples of the glass/SiC and alumina/SiC/glass composites sintered at 1000°C and on solid samples of the alumina/SiC/glass sintered and hot-pressed at 1600°C and 70 MPa (10,000 psi). The results of the x-ray diffraction analysis are shown in Figures 20-26. Composites containing each sintering aid retained some glass phase at a sintering temperature of 1000°C, however at the final sintering and hot-pressing conditions, minimal residual glass phase can be seen in the x-ray diffraction plots.

The phases identified in the composites are similar to what would be expected from study of the ternary phase diagrams in Figures 3 and 4. Exact comparison is not possible however, as the sintering aids are actually quaternary systems. X-ray diffraction identified phases containing the fourth component, TiO₂. The presence of 85 wt% alumina may also have masked peaks associated with minor crystalline phases.

XRD of LAS Glass w/SiC
Sintered at 1000 C

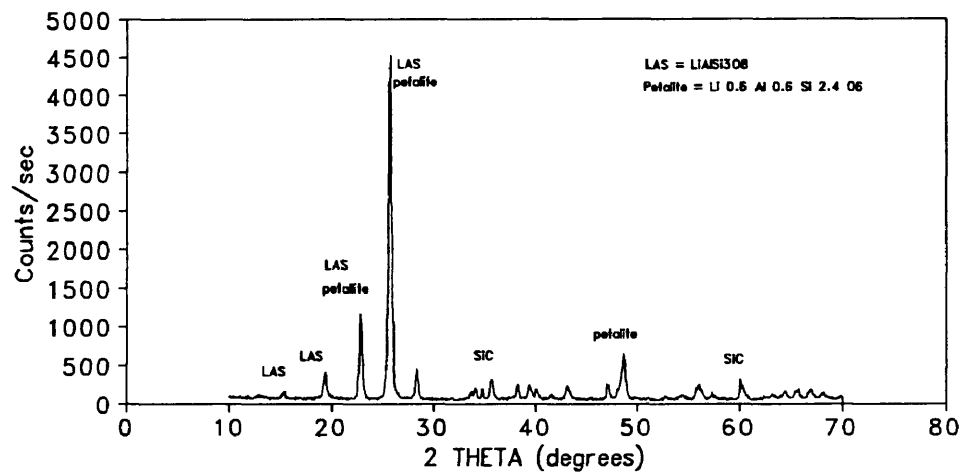


Figure 20 X-ray diffraction pattern of LAS/SiC sintered at 1000°C.

XRD of Al₂O₃/LAS/SiC
Sintered at 1000 C

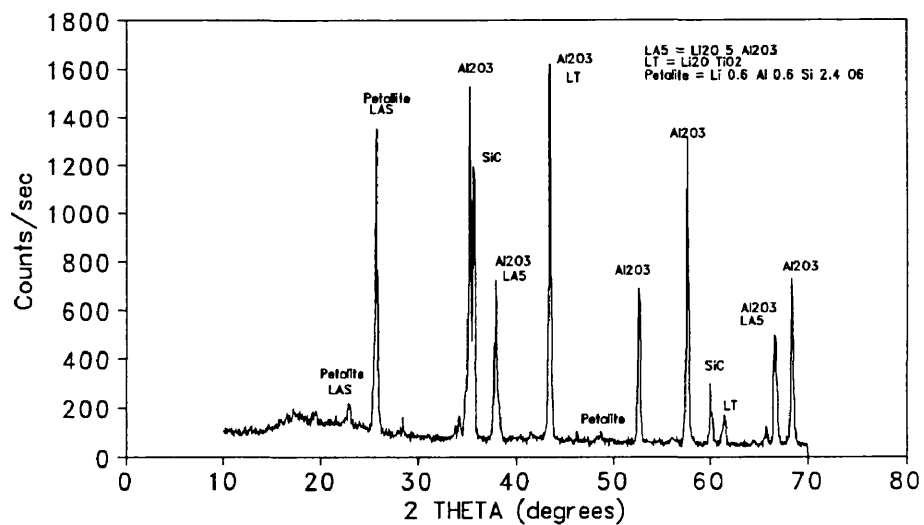


Figure 21 X-ray diffraction of alumina/SiC/LAS sintered at 1000°C.

XRD of Al₂O₃/LAS/SiC
Sintered at 1600 C and 10Kpsi

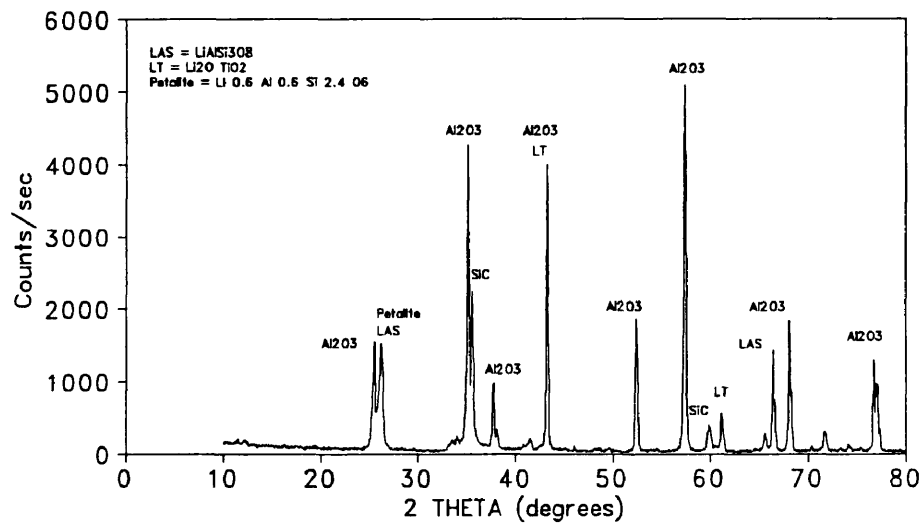


Figure 22 X-ray diffraction of alumina/SiC/LAS hot-pressed at 1600°C and 70 MPa (10,000 psi).

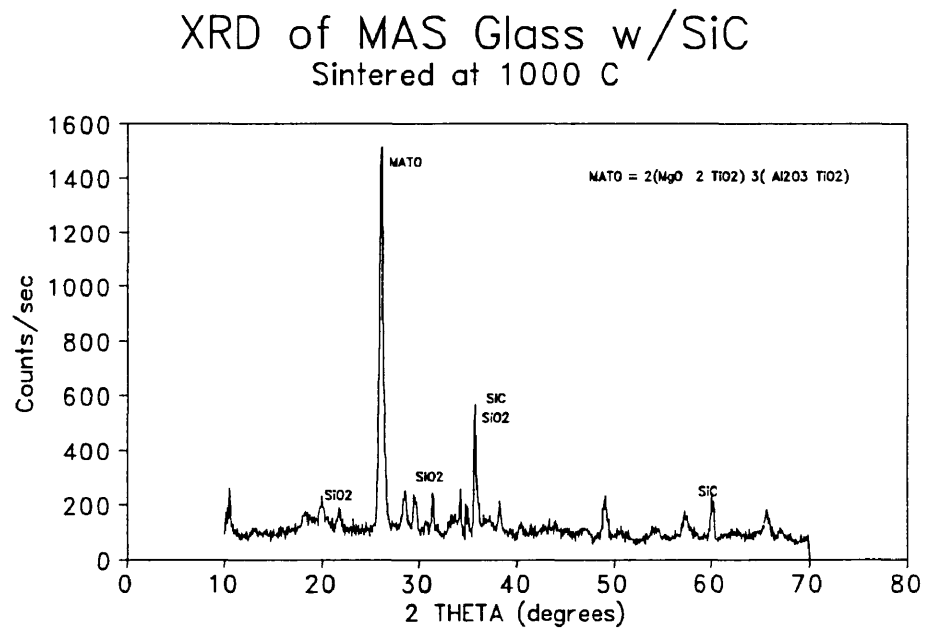


Figure 23 X-ray diffraction of MAS/SiC sintered at 1000°C.

XRD of Al₂O₃/MAS/SiC
Sintered at 1000 C

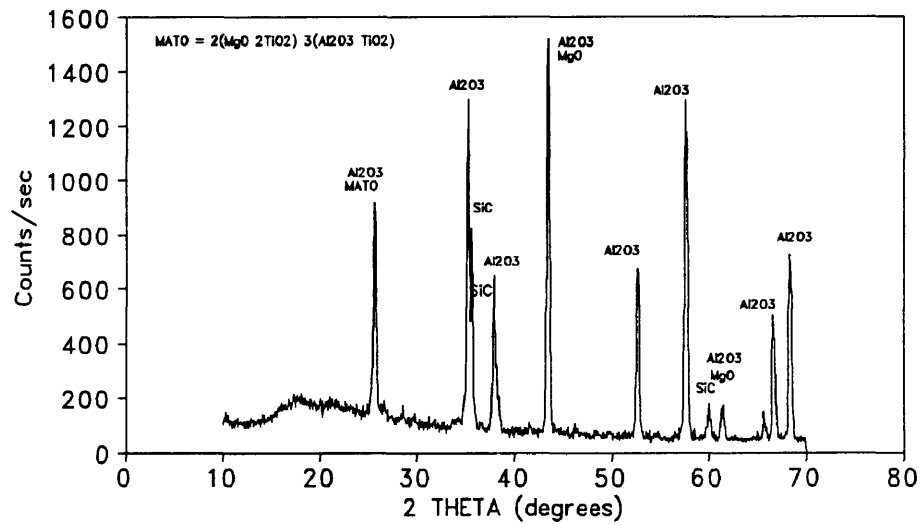


Figure 24 X-ray diffraction of alumina/SiC/MAS sintered at 1000°C.

XRD of Al₂O₃/SiC/MAS Sintered at 1600 C 10Kpsi

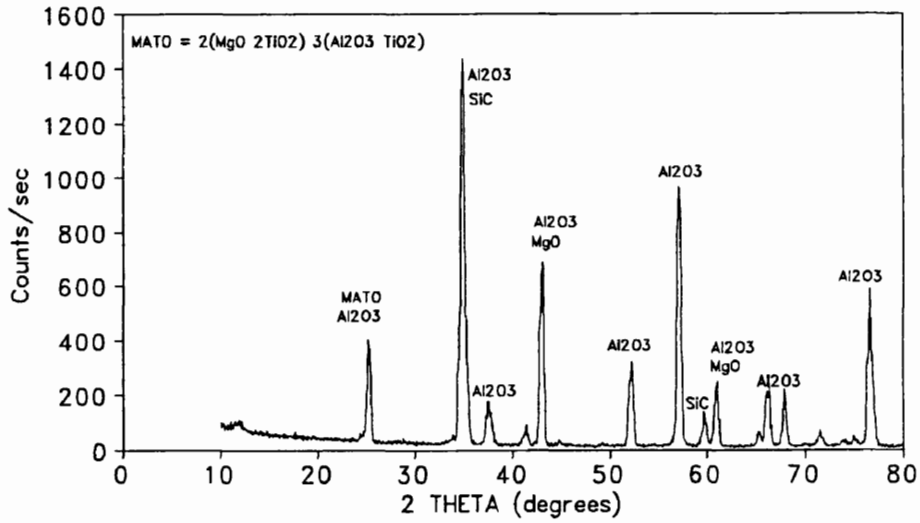


Figure 25 X-ray diffraction of alumina/SiC/MAS hot-pressed at 1600°C and 70 MPa (10,000 psi).

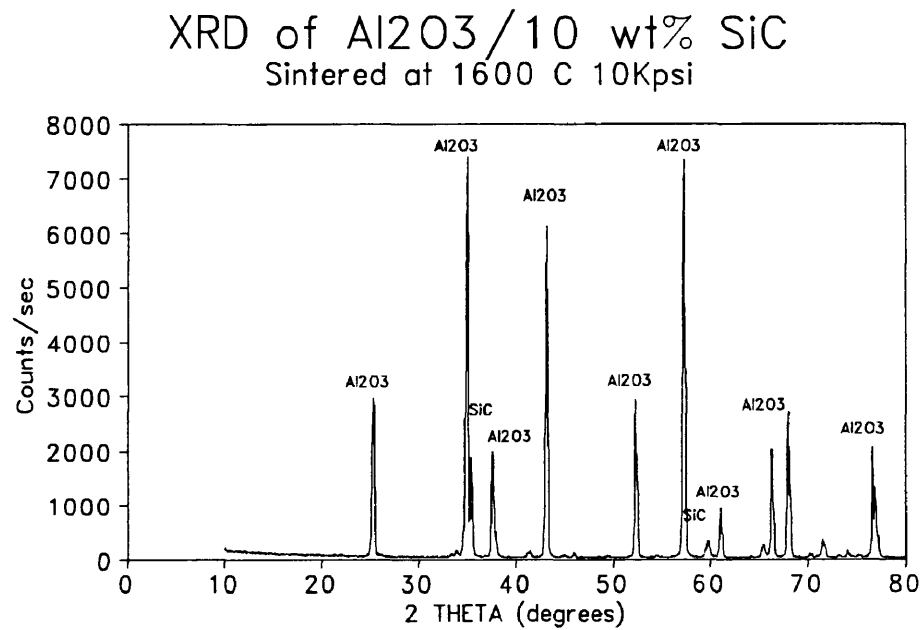


Figure 26 X-ray diffraction of alumina/SiC hot-pressed at 1600°C and 70 MPa (10,000 psi).

4.4 Densification of Alumina/SiC Composites by Sintering Aids

The addition of sintering aids increased the density of the alumina/SiC/glass composites to 97% of theoretical density. The density of the alumina/SiC composite without a sintering aid was also determined to be 98% of theoretical density. The micrographs presented in section 4.2 show the amount of porosity decreased with increased sintering temperature and, in the case of alumina/SiC without the sintering aids, the porosity was concentrated around the platelets. Figure 27 presents the percent of theoretical density, as determined by the Archimedes method, of each composite manufactured. Actual data are contained in Appendix B.

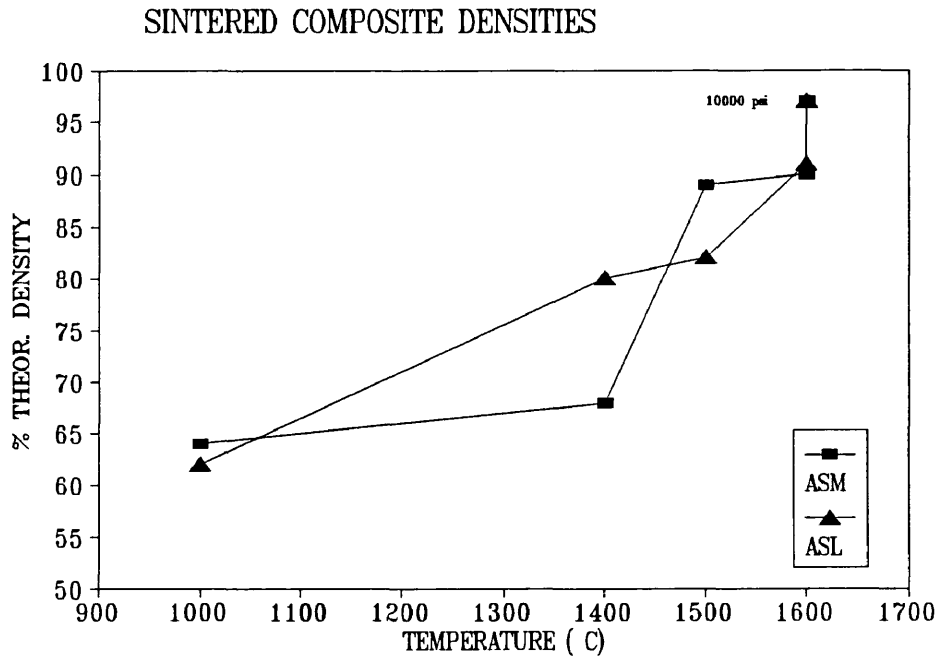


Figure 27 Density (as % of theoretical density) of alumina/SiC/glass composites.

CHAPTER 5

CONCLUSIONS

Two non-reactive glass sintering aid compositions, lithia-alumina-silicate and magnesia-alumina-silicate, were developed to improve the sinterability of alumina/SiC composites. Thermodynamic modelling predicted the possibility of reaction between the lithia and magnesia with the silicon carbide. No evidence of conversion of the silicon carbide to silica was found in the microstructural SEM examination or in the x-ray diffraction analysis of samples sintered and hot-pressed at 1600°C and 70 MPa (10,000 psi).

The sintering aid selection criteria also specified that the sintering aid should easily devitrify, leaving no glassy phase which could decrease the room temperature and high temperature mechanical strength of the composite. X-ray diffraction analysis of the hot-pressed composites detected no residual glass in the samples.

The density of composites with either sintering aid achieved 97% of theoretical density at 1600°C and 70 MPa (10,000 psi). The mechanical properties of the composite were not tested in this study.

Future Investigation

Areas for future study in this composite system should include the measuring of the mechanical properties of the material to compare the composites prepared with a sintering aid to the properties of alumina/SiC platelet and whisker composites with no sintering aid and with other types of sintering aids. The mechanical properties should be measured at both room temperature and at higher temperature ($> 1000^{\circ}\text{C}$). Properties to be determined include: fracture strength, toughness, thermal expansion and thermal conductivity.

Processing of the alumina/SiC/glass composites requires optimization. This includes increasing the platelet loading, which other researchers have found to be optimal at 20 wt% in whisker composites. The material also should be processed by HIPping, which will allow the manufacture of more complex parts at lower cost.

The composition of the sintering aids was based on the ternary phase relationships of the lithia or magnesia with alumina and silica. The nucleating agent, TiO_2 , was based on compositions of glass-ceramics in the literature. Therefore, the compositions of the sintering aids could be optimized.

The kinetics of the reactions between SiC and oxides in glassy phase should be investigated to determine whether the difference in the thermodynamic model predictions is due to the kinetics of the reaction and mass transfer within the system, or if the discrepancy is the result of inaccuracies in the thermodynamic data available for oxides and carbides at high temperatures.

REFERENCES

1. J. D. Birchall, D. R. Stanley, M. J. Mockford, "Toxicity of Silicon Carbide Whiskers", *Journal of Material Science Letters*, **7** 350-352 (1988).
2. L. M. Sheppard, "Cost Effective Manufacturing of Advanced Ceramics", *Ceramic Bulletin*, **70** [4] 692-701 (1991).
3. T. N. Tiegs and D. M. Dillard, "Effect of Aspect Ratio and Liquid-Phase Content on Densification of Alumina-Silicon Carbide Whisker Composites", *Journal of the American Ceramics Society*, **73** [5] 1440-1442 (1990).
4. D. Baril and M. K. Jain, "Evaluation of SiC Platelets as a Reinforcement for Oxide Matrix Composites", private communication.
5. Information from Coors Porcelain Company, Golden, Colorado sales brochure.
6. W. A. Zdaniewski and H. P. Kirchner, "Toughening of a Sintered Alumina by Crystallization of the Grain Boundary Phase", *Advanced Ceramic Materials*, **1** [1] 99-103 (1986).
7. S. M. Weiderhorn, B. J. Hockey, and R. F. Krause Jr., "Influence of Microstructure on Creep Rupture", *Ceramic Microstructures '86*, Ed. J. A. Pask and A. G. Evans, Plenum Press, New York, 795-806 (1987).
8. L. M. Sheppard, "Ceramics at the 'Cutting Edge'", *Advanced Materials and Processes*, 8/87, 73-8.
9. Guide to Selecting Engineering Materials, *Advanced Materials and Processes*, June 1987 supplement.
10. P. F. Becher and G. C. Wei, "Toughening Behavior of SiC-Whisker Reinforced Alumina", *Journal of the American Ceramic Society*, Dec., C - 267-269 (1984).
11. T. N. Tiegs and P. F. Becher, "Sintered Al₂O₃-SiC-Whisker Composites", *Ceramic Bulletin*, **66** [2] 339-42 (1987).

12. I. B. Cutler, C. Bradshaw, C. J. Christensen and E. P. Hyatt, "Sintering of Alumina at Temperatures of 1400°C and Below", *Journal of the American Ceramic Society*, **40** [4], 134-139 (1957).
13. M. Harmer, E. W. Roberts and R. J. Brooks, "Rapid Sintering of Pure and Doped α -Al₂O₃", *Transactions of the British Ceramic Society*, **78** [1] 22-25 (1979).
14. T. Ikegami, K. Kotani and K. Eguchi, "Some Roles of MgO and TiO₂ in the Densification of a Sinterable Alumina", *Journal of the American Ceramic Society*, **70** [12] 885-90 (1987).
15. T. K. Brog, private communication, 1989.
16. D. Popoola and A. H. Heuer, "Microstructural and Microchemical Analysis of Al₂O₃/SiC HIPped Composites" and "Microstructural Studies of Al₂O₃/SiC and Al₂O₃/SiC MnO₂-TiO₂ Composites", unpublished research reports for Coors Ceramics, 1989.
17. P. W. McMillan, "Glass-Ceramics", Academic Press, New York, 58 (1979).
18. E. M. Levin, C. R. Robbins, and H. F. McMurdie, eds., Phase Diagrams for Ceramists, Vol. 2, 2464 (1969).
19. E. M. Levin, C. R. Robbins, and H. F. McMurdie, eds., Phase Diagrams for Ceramists, Vol. 1, 712 (1964).
20. W. D. Kingery, H. K. Bowen, D. R. Uhlman, Introduction to Ceramics, John Wiley and Sons, New York, 92-97 (1976).
21. W. J. Zachariasen, "The Atomic Arrangement in Glass", *Journal of the American Chemical Society*, **54** [10] 3841-51 (1932).
22. S. M. Wiederhorn, B. J. Hockey, R. F. Krause Jr. and K. Jakus, "Creep and Fracture of a Vitreous-Bonded Aluminum Oxide", *Journal of Material Science*, **21** 810-24 (1986).
23. L. B. Pankratz, Thermodynamic Properties of Elements and Oxides, Bulletin 672, U. S. Dept. of the Interior and Bureau of Mines,
24. D. R. Stull and H. Prephet, JANAF Thermochemical Tables, 2nd. Edition, National Bureau of Standards, Washington, DC. (1971).

25. G. Eriksson, "Thermodynamic Studies of High Temperature Equilibrium; XII SOLGASMIX, a computer program for calculation of equilibrium compositions in multiphase systems", *Chemica Scripta*, **8**, (1975) 100-103.
26. K. M. Prewo and J. J. Brennan, "High-Strength Silicon Carbide Fibre-Reinforced Glass-Matrix Composites", *Journal of Material Science*, **15** [2] 463-68 (1980).
27. J. J. Brennan, "Interfacial Chemistry and Bonding in Fiber Reinforced Glass and Glass-Ceramic Matrix Composites", *Ceramic Microstructure '86*, Proceedings of the 22 University Conference of Ceramics and the International Materials Symposium, July 1986, Material Science Research [21] Plenum Press, New York, 387-99 (1987).
28. R. Chaim and A. H. Heuer, "The Interface Between (Nicalon) SiC Fibers and a Glass-Ceramic Matrix", *Advanced Ceramic Materials*, **2** [2] 154-58 (1987).
29. R. F. Cooper and K. Chung, "Structure and Chemistry of Fibre-Matrix Interfaced in Silicon Carbide Fibre-Reinforced Glass-Ceramic Composites: an Electron Microscopy Study", *Journal of Materials Science*, **22** 3148-60 (1987).
30. E. Bishcoff, M. Ruhle, O. Sbaizero, and A. G. Evans, "Microstructural Studies of the Interfacial Zone of a SiC-Fiber-Reinforced Lithium Aluminum Silicate Glass-Ceramic", *Journal of the American Ceramics Society*, **72** [5] 741-45 (1989).
31. T. J. P. Lewis, Temperature Determination in an Inductively Heated Graphite Die Using Finite Element Methods, Colorado School of Mines, Golden, Colorado, #T-3985 (January 1991).

APPENDIX A
THERMODYNAMIC MODELLING CALCULATIONS

CALCULATION OF GIBBS FREE ENERGIES

| REACTIONS | | TEMP. (K) | 1000 | 1200 | 1400 | 1600 | 1800 | 2000 |
|-----------|---|--------------------------|----------|----------|----------|----------|----------|----------|
| (1) | $\text{SiC (s)} = \text{Si (s)} + \text{C (s)}$ | $-\Delta G =$ | 63.517 | 61.972 | 60.432 | 58.888 | 53.912 | 46.432 |
| | $\text{Si (s)} + \text{O}_2(\text{g}) = \text{SiO}_2(\text{qu})$ | $\Delta G =$ | -730.79 | -696.163 | -661.758 | -627.637 | -590.132 | -550.359 |
| (2) | $\text{SiC (s)} + \text{O}_2(\text{g}) = \text{SiO}_2(\text{qu}) + \text{C (s)}$ | $\Delta G(\text{rxn}) =$ | -667.273 | -634.191 | -601.326 | -568.749 | -536.220 | -503.927 |
| | $2/3[\text{SiC (s)} = \text{Si (s)} + \text{C (s)}]$ | $-2/3 \Delta G =$ | 42.344 | 41.3146 | 40.288 | 39.258 | 35.941 | 30.954 |
| | $2/3[\text{Si (s)} + \text{O}_2(\text{g}) = \text{SiO}_2(\text{qu})]$ | $2/3 \Delta G =$ | -487.193 | -464.108 | -441.172 | -418.425 | -393.421 | -366.906 |
| | $2/3[\text{C (s)} + 1/2 \text{O}_2(\text{g}) = \text{CO (g)}]$ | $2/3 \Delta G =$ | -133.489 | -145.176 | -156.724 | -168.138 | -179.440 | -190.631 |
| (3) | $2/3 \text{SiC (s)} + \text{O}_2(\text{g}) = 2/3 \text{SiO}_2(\text{qu}) + 2/3 \text{CO (g)}$ | $\Delta G(\text{rxn}) =$ | -578.337 | -567.970 | -557.608 | -547.304 | -536.920 | -526.582 |
| | $1/2[\text{SiC (s)} = \text{Si (s)} + \text{C (s)}]$ | $-1/2 \Delta G =$ | 31.758 | 30.986 | 30.216 | 29.444 | 26.956 | 23.216 |
| | $1/2[\text{Si (s)} + \text{O}_2(\text{g}) = \text{SiO}_2(\text{qu})]$ | $1/2 \Delta G =$ | -365.395 | -348.081 | -330.879 | -313.818 | -295.066 | -275.179 |
| | $1/2[\text{C (s)} + \text{O}_2(\text{g}) = \text{CO}_2(\text{g})]$ | $1/2 \Delta G =$ | -197.942 | -198.047 | -198.120 | -198.164 | -198.177 | -198.171 |
| (4) | $1/2 \text{SiC (s)} + \text{O}_2(\text{g}) = 1/2 \text{SiO}_2(\text{qu}) + 1/2 \text{CO (g)}$ | $\Delta G(\text{rxn}) =$ | -531.579 | -515.143 | -498.783 | -482.539 | -466.287 | -450.134 |
| | $\text{SiC (s)} = \text{Si (s)} + \text{C (s)}$ | $-\Delta G =$ | 63.517 | 61.972 | 60.432 | 58.888 | 53.912 | 46.432 |
| | $\text{Si (s)} + 1/2 \text{O}_2(\text{g}) = \text{SiO (g)}$ | $\Delta G =$ | -186.455 | -202.719 | -218.655 | -234.396 | -246.346 | -255.659 |
| | $\text{C (s)} + 1/2 \text{O}_2(\text{g}) = \text{CO (g)}$ | $\Delta G =$ | -200.233 | -217.764 | -235.086 | -252.207 | -269.160 | -285.947 |
| | $\text{SiC (s)} + \text{O}_2(\text{g}) = \text{SiO (g)} + \text{CO (g)}$ | $\Delta G(\text{rxn}) =$ | -323.172 | -358.511 | -393.310 | -427.715 | -461.594 | -495.174 |

continued

| REACTIONS | | TEMP. (K) | 1000 | 1200 | 1400 | 1600 | 1800 | 2000 |
|---|--|--------------------------|----------|----------|----------|----------|----------|----------|
| (5) | $2\text{SiC}(s) = \text{Si}(s) + \text{C}(s)$ | $-2 \Delta G =$ | 127.034 | 123.944 | 120.864 | 117.776 | 107.824 | 92.864 |
| | $2\text{C}(s) + 1/2 \text{O}_2(g) = \text{CO}(g)$ | $2 \Delta G =$ | -400.467 | -435.529 | -470.173 | -504.415 | -538.322 | -571.894 |
| | $2\text{SiC}(s) + \text{O}_2(g) = 2\text{Si}(s) + 2\text{CO}(g)$ | $\Delta G(\text{rxn}) =$ | -273.433 | -311.585 | -349.309 | -386.639 | -430.498 | -479.030 |
| (6) | $2\text{SiC}(s) = \text{Si}(s) + \text{C}(s)$ | $-2 \Delta G =$ | 127.034 | 123.944 | 120.864 | 117.776 | 107.824 | 92.864 |
| | $2\text{Si}(s) + 1/2 \text{O}_2(g) = \text{SiO}(g)$ | $2 \Delta G =$ | -372.912 | -405.438 | -437.312 | -468.792 | -492.691 | -511.318 |
| | $2\text{SiC}(s) + \text{O}_2(g) = 2\text{SiO}(g) + 2\text{C}(s)$ | $\Delta G(\text{rxn}) =$ | -245.878 | -281.494 | -316.448 | -351.016 | -384.870 | -418.454 |
| (7) | $\text{SiC}(s) = \text{Si}(s) + \text{C}(s)$ | $-\Delta G =$ | 63.517 | 61.972 | 60.432 | 58.888 | 53.912 | 46.432 |
| | $\text{C}(s) + \text{O}_2(g) = \text{CO}_2(g)$ | $\Delta G =$ | -395.885 | -396.095 | -396.241 | -396.329 | -396.354 | -396.342 |
| | $\text{SiC}(s) + \text{O}_2(g) = \text{Si}(s) + \text{CO}_2(g)$ | $\Delta G(\text{rxn}) =$ | -332.368 | -334.123 | -335.809 | -337.441 | -342.442 | -349.91 |
| (8) | $2/3\text{SiC}(s) = \text{Si}(s) + \text{C}(s)$ | $-2/3 \Delta G =$ | 42.344 | 41.314 | 40.288 | 39.258 | 35.941 | 30.954 |
| | $2/3\text{Si}(s) + 1/2 \text{O}_2(g) = \text{SiO}(g)$ | $2/3 \Delta G =$ | -124.303 | -135.146 | -145.770 | -156.264 | -164.230 | -170.439 |
| | $2/3\text{C}(s) + \text{O}_2(g) = \text{CO}_2(g)$ | $2/3 \Delta G =$ | -263.923 | -264.063 | -264.161 | -264.219 | -264.236 | -264.228 |
| $2/3\text{SiC}(s) + \text{O}_2(g) = 2/3\text{SiO}(g) + 2/3\text{CO}_2(g)$ | $\Delta G(\text{rxn}) =$ | -345.883 | -357.894 | -369.643 | -381.225 | -392.525 | -403.712 | |

GIBBS FREE ENERGY DATABASE

REACTIONS

| TEMP (K) | | ΔG OF COMPOUNDS (kJ/mol) | | | | | | | | | |
|-------------|--------------------------|----------------------------------|----------|---------|----------|----------|---------|----------|---------|--|--|
| | | Al | Zr | Ti | Mn | Si | Li | Ca | Mg | | |
| 1000 | $\Delta G(\text{car}) =$ | -169.80 | -188.00 | -172.65 | -701.592 | -63.517 | -104.35 | -531.007 | 59.68 | | |
| | $\Delta G(\text{ox}) =$ | -1361.46 | -910.15 | -762.25 | -1.255 | -667.273 | -465.61 | -20.719 | -493.15 | | |
| | $\Delta G(\text{oc}) =$ | -1531.26 | -1098.14 | -934.90 | -702.85 | -730.790 | -569.96 | -551.73 | -433.47 | | |
| 1200 | $\Delta G(\text{car}) =$ | -150.77 | -186.64 | -170.32 | -650.598 | -61.972 | -121.28 | -509.696 | 51.93 | | |
| | $\Delta G(\text{ox}) =$ | -1295.20 | -873.11 | -726.96 | -1.602 | -643.119 | -438.27 | -21.984 | -469.96 | | |
| | $\Delta G(\text{oc}) =$ | -1445.97 | -1059.75 | -897.28 | -652.20 | -705.091 | -559.54 | -531.68 | -418.03 | | |

continued

| TEMP (K) | ΔG OF COMPOUNDS (kJ/mol) | | | | | | | | | |
|-------------|----------------------------------|----------|----------|---------|----|----------|---------|----|--|---------|
| | Al | Zr | Ti | Mn | Si | Li | Ca | Mg | | |
| 1400 | $\Delta G(\text{car}) =$ | -131.24 | -184.88 | -167.32 | | -60.432 | -140.23 | | | 46.64 |
| | $\Delta G(\text{ox}) =$ | -1229.31 | -836.02 | -691.38 | | -601.326 | -411.40 | | | -443.33 |
| | $\Delta G(\text{oc}) =$ | -1360.55 | -1020.89 | -858.70 | | -661.758 | -551.63 | | | -396.69 |
| 1600 | $\Delta G(\text{car}) =$ | -111.31 | -183.18 | -164.31 | | -58.888 | -160.96 | | | 56.04 |
| | $\Delta G(\text{ox}) =$ | -1163.81 | -799.95 | -656.05 | | -568.75 | -385.04 | | | -401.78 |
| | $\Delta G(\text{oc}) =$ | -1275.12 | -983.13 | -820.36 | | -627.638 | -546.00 | | | -345.74 |
| 1800 | $\Delta G(\text{car}) =$ | -91.04 | -181.52 | -161.25 | | -50.168 | -167.19 | | | 64.54 |
| | $\Delta G(\text{ox}) =$ | -1098.66 | -764.57 | -620.93 | | -536.22 | -330.21 | | | -360.32 |
| | $\Delta G(\text{oc}) =$ | -1189.70 | -946.09 | -782.18 | | -586.388 | -497.40 | | | -295.78 |
| 2000 | $\Delta G(\text{car}) =$ | -70.49 | -179.85 | -157.67 | | -46.432 | -173.25 | | | 72.22 |
| | $\Delta G(\text{ox}) =$ | -1033.86 | -729.38 | -585.58 | | -503.927 | -269.51 | | | -319.74 |
| | $\Delta G(\text{oc}) =$ | -1104.35 | -909.23 | -743.25 | | -550.359 | -442.76 | | | -247.52 |

REF. OXIDES: BULLETIN 672; CARBIDES: JANAF TABLES

APPENDIX B

CALCULATION OF % THEORETICAL DENSITY

1) Weight Percent Density Estimation of Oxide Composites

Density of Composite Components - from CRC Handbook of Chemistry and Physics,
54th edition.

| | | |
|--------------------------------|---|------------|
| Al ₂ O ₃ | = | 3.965 g/cc |
| Li ₂ O | = | 2.013 |
| MgO | = | 3.58 |
| SiC | = | 3.217 |
| SiO ₂ | = | 2.635 |
| TiO ₂ | = | 4.17 |

Density of LAS

| | | |
|---|---|-----------|
| 5 wt% Li ₂ O * 2.013 | = | 0.101 |
| 20 wt% Al ₂ O ₃ * 3.965 | = | 0.793 |
| 70 wt% SiO ₂ * 2.635 | = | 1.845 |
| 5 wt% TiO ₂ * 4.17 | = | 0.21 |
| ----- | | |
| | | 2.95 g/cc |

Density of MAS

| | | |
|---|---|-----------|
| 15 wt% MgO * 3.58 | = | 0.54 |
| 30 wt% Al ₂ O ₃ * 3.965 | = | 1.19 |
| 45 wt% SiO ₂ * 2.635 | = | 1.19 |
| 10 wt% TiO ₂ * 4.17 | = | 0.42 |
| ----- | | |
| | | 3.34 g/cc |

Density of ASM

$$\begin{array}{rcl} 85 \text{ wt\% Al}_2\text{O}_3 * 3.965 & = & 3.37 \\ 10 \text{ wt\% SiC} * 3.217 & = & 0.32 \\ 5 \text{ wt\% MAS} * 3.34 & = & 0.17 \\ \hline & & 3.86 \text{ g/cc} \end{array}$$

Density of ASL

$$\begin{array}{rcl} 85 \text{ wt\% Al}_2\text{O}_3 * 3.965 & = & 3.37 \\ 10 \text{ wt\% SiC} * 3.217 & = & 0.32 \\ 5 \text{ wt\% LAS} * 2.95 & = & 0.15 \\ \hline & & 3.84 \text{ g/cc} \end{array}$$

2) Density Estimation of Glasses¹

$$\text{Calculate } N_{\text{Si}}: N_{\text{Si}} = f_{\text{Si}} / 60.06(s_1f_1 + s_2f_2 + \dots)$$

$$\text{where } f_x = \text{wt\% of } x/100$$

$$s_x = \# \text{ O atoms/MW of } x$$

$$\text{LAS: } N_{\text{Si}} = 0.363$$

$$\text{MAS: } N_{\text{Si}} = 0.250$$

Using N_{Si} and Table 20-2 from Huggins, obtain the specific volume factor, v_x .

$$\text{Calculate density: } 1/d = (v_1f_1 + v_2f_2 + \dots)$$

$$\text{LAS: } d = 2.395$$

$$\text{MAS: } d = 2.422$$

¹ Huggins, M. L. and K. H. Sun, "Calculation of Density and Optical Constants of a Glass From Its Composition in Weight Percentage", J. Amer. Cer. Soc., Vol 21 [1], 1943, pp. 4-11.

% Theoretical Density = $100 * \text{bulk solid density } (D_b) / \text{theoretical density } (D_{th})$

$$\text{bulk density} = W_{dry} / \text{vol}_{bulk}$$

$$\text{vol}_{bulk} = (W_{sat} - W_{susp} - W_{wire}) / \text{specific gravity of fluid}$$

$$W_{dry} = \text{weight of bulk solid}$$

$$W_{sat} = \text{weight of solid} + \text{weight of fluid filling open pores}$$

$$W_{susp} = \text{weight of air filling closed pores}$$

$$W_{wire} = \text{weight of wire used to suspend sample in fluid}$$

| COMPOSITE | TEMP. (°C) | W_{dry} (g) | W_{sat} (g) | W_{susp} (g) | D_b (g/cc) | % D_{th} |
|-------------------------------------|---------------|------------------|------------------|-------------------|-----------------|------------|
| ASM | 1000 | 2.4920 | 2.8455 | 1.8369 | 2.47 | 64 |
| | 1400 | 1.3293 | 104803 | 0.9705 | 2.61 | 68 |
| | 1500 | 1.3163 | 1.3230 | 0.9542 | 3.57 | 92 |
| | 1500 | 1.8838 | 1.9270 | 1.3670 | 3.37 | 87 |
| | 1600 | 2.4309 | 2.4795 | 1.7822 | 3.49 | 90 |
| | 1600 HP | 0.5777 | 0.5796 | 0.4255 | 3.75 | 97 |
| ASL | 1000 | 1.0750 | 1.2330 | 0.7843 | 2.40 | 62 |
| | 1400 | 1.3874 | 1.4450 | 0.9965 | 3.09 | 80 |
| | 1500 | 1.6626 | 1.7060 | 1.1858 | 3.20 | 83 |
| | 1500 | 1.0277 | 1.0720 | 0.7389 | 3.09 | 80 |
| | 1600 | 1.0390 | 1.1173 | 0.8025 | 3.51 | 91 |
| | 1600 HP | 0.7098 | 0.7142 | 0.5243 | 3.74 | 97 |
| Al ₂ O ₃ /SiC | 1600 HP | 0.7327 | 0.7349 | 0.5421 | 3.80 | 98 |